

Kathrin.Ballweg@gris.tu-darmstadt.de m.schaepers1993@gmail.com margit.pohl@tuwien.ac.at
andreas.kerren@liu.se landesberger@cs.uni-koeln.de

A Shape Change Enhancing Hierarchical Layout for the Pairwise Comparison of Directed Acyclic Graphs

Kathrin Guckes (née Ballweg)¹, Marc Schäpers¹, Prof. Margit
Pohl², Prof. Andreas Kerren⁴, and Prof. Tatiana von
Landesberger³

¹Graphical Interactive Systems Group, Technical University
Darmstadt

²Informatics, TU Wien

³Visualisierung und Visual Analytics, University of Cologne

⁴Information Visualization Group, Linköping University

June 11, 2024

Abstract

Comparing directed acyclic graphs (DAGs) is essential in various fields such as healthcare, social media, finance, biology, and marketing. DAGs often result from contagion processes over networks, including information spreading, retweet activity, disease transmission, financial crisis propagation, malware spread, and gene mutations. For instance, in disease spreading, an infected patient can transmit the disease to contacts, making it crucial to analyze and predict scenarios. Similarly, in finance, understanding the effects of saving or not saving specific banks during a crisis is vital.

Experts often need to identify small differences between DAGs, such as changes in a few nodes or edges. Even the presence or absence of a single edge can be significant. Visualization plays a crucial role in facilitating these comparisons. However, standard hierarchical layout algorithms struggle to visualize subtle changes effectively.

The typical hierarchical layout, with the root on top, is preferred due to its performance in comparison to other layouts. Nevertheless, these standard algorithms prioritize single-graph aesthetics over comparison suitability, making it challenging for users to spot changes.

To address this issue, we propose a layout that enhances shape changes in DAGs while minimizing the impact on aesthetics. Our approach involves outwardly swapping changes, altering the DAG's shape. We introduce new drawing criteria:

1. Criteria for maximizing outward swaps of graph changes.

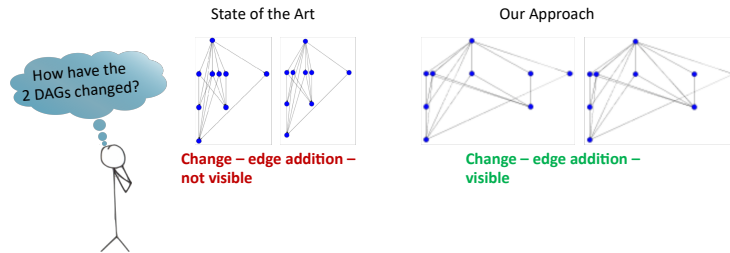


Figure 1: Motivational example – shape changes of the directed acyclic graphs ease their pairwise visual comparison.

2. Criteria for reshaping the DAG by repositioning swapped changes.
3. Criteria for handling changes that cannot be outwardly swapped.


Our layout builds upon a Sugiyama-like hierarchical layout and implements these criteria through two extensions. We designed it this way to maintain interchangeability and accommodate future optimizations, such as pseudo-nodes for edge crossing minimization.

In our evaluations, our layout achieves excellent results, with edge crossing aesthetics averaging around 0.8 (on a scale of 0 to 1). Additionally, our layout outperforms the base implementation by an average of 60 – 75%.



1 Introduction

Visual comparison of DAGs is a task encountered in various disciplines, e.g., in healthcare, social media, finance, biology, or marketing. Directed acyclic graphs often result from so-called contagion processes over networks, that is information spreading and retweet activity [17, 90, 8, 86], disease spreading [1, 73], financial crisis propagation [87, 75], malware propagation in computer networks [61], or gene mutations [58]. For example, in disease spreading, an infected patient may transmit the disease to the patients, who were in contact with her. Those contact persons, in turn, may transmit the disease to their contacts along the social network. This is currently a lively topic in healthcare. There, medical experts analyze, predict, and compare spreading scenarios [39, 43]. In all of these applications, it is often crucial to compare two scenarios, for instance, the comparison of two disease spreading scenarios – 1) with and 2) without patient isolation [89, 43]. Or in the case of social media analysis, social media experts are interested in human retweeting behavior for two different message types. Necessary comparisons for financial crisis propagation analysis may be the effects of saving or not saving specific banks on the crisis contagion [87]. The domain experts need to identify even small differences between DAGs, i.e., changes of few nodes and/or edges may be crucial. The presence or absence of just one edge, as in the motivating example shown in Figure 1, can have a significant impact. For disease spreading, it may determine whether an entire

hospital ward needs to be isolated or whether an entire school or entire country needs to be isolated as we experienced it with the Corona virus. Also reaching a certain recipient of a tweet may decide upon whether a tweet goes viral or not.

Visualization often supports such comparisons of DAGs. In this case, it is the visualization’s job to convey the differences between the two DAGs. Differences, also called changes, may be nodes and/or edges which have been added and/or deleted. As our motivational example of Figure 1 shows, even for small graphs, the visualization of changes is difficult – especially of subtle ones like the addition of a single edge to the inner structure of the visualized DAG. As Figure 1 shows, standard hierarchical layout algorithms have a troubles visualizing such changes so that they are well spottable. By standard hierarchical layout algorithms we mean layout algorithms which follow the drawing principles of the Sugiyama layout [82] and respect the common graph drawing aesthetics to achieve a well-readable drawing result [24, 83, 62, 26, 71, 9, 25, 13]. We decided for a standard hierarchical node-link diagram layout with the root placed on top () , since Burch et al. [20, 19] found that this layout type outperforms other types such as orthogonal or radial layouts. The problems of these standard Sugiyama-like algorithms are readily understood. The optimizations and aesthetics they consider, except for mental map stability, are not designed for comparison but for visualization of a single graph – DAG. The mental map stability helps to prevent the position of the remaining graph elements from changing too much, thus making the comparison even more complicated for humans. However, it has no influence directly on the visualizations of the changes in the DAGs. So, this means we need optimizations that take into account comparison aspects such as good change detectability. To the best of our knowledge, such optimizations for the good detectability of changes in DAGs do not currently exist.

A fair question is: “Why not just highlight the the DAG’s changes?” The answer to this questions is: it is not as easy as it seems. Scenarios where color as a visual variable is needed for other information are likely. Often graph-structured data has additional attributes like nodes or edge categories (cf. e.g., [49]) and color is one of the most suited visual variable for such information [16]. So, it would be really beneficial to have another visual mapping for the DAGs’ changes.

In our study on visual comparisons with respect to commonalities [11, 12], we found that humans are sensitive to small variations in shape. They denoted DAGs like this  as “narrow pyramids” and DAGs like this  as “wide pyramids”. So, why do we not just exploit the human sensitive notion of shape for improving the detectability of DAG changes in the context of pairwise visual comparisons? Figure ?? visualizes the idea: Instead of not paying particular attention to the positioning of the changing graph elements, our idea is to outwardly swap as many changes as possible, taking into account the graph drawing aesthetics, thus changing the shape of the DAG. But this needs new drawing criteria:

- We need drawing criteria which lead to outwardly swapping as many graph changes as possible.

- We need drawing criteria which lead to shape changes by repositioning the outwardly swapped DAG changes.
- We need criteria which deal with DAG changes which are not possible to outwardly swap – nevertheless we also need a change of the DAG’s shape for those as well.

We propose a shape change enhancing layout which implements the above criteria based on two extensions of a Sugiyama-like hierarchical layout. Our layout performs the shape change enhancements so that the influence on graph aesthetics is as small as possible. We decided to implement the novel criteria extension-based to allow for the interchangeability of the Sugiyama-like layout on which we based our layout. Interchanging the base Sugiyama-like layout may be necessary in case of further optimizations – e.g., pseudo-nodes for further edge crossing minimization – are needed. In our case with employing the barycenter edge crossing minimization method, further edge crossing minimization was not needed since on average we achieve values of around 0.8 for the edge crossing aesthetic. These are very good results since a value 1 is the highest possible value. Furthermore, our evaluation shows that our layout outperforms the base implementation, on average, in 60 – 75%.

1.1 Related Work

Since we propose a shape change enhancing layout for the pairwise visual comparison of DAGs which fosters the detectability of changes for humans by changing the DAG shape, our work is located in these research areas:

- Static graph drawing resp. layouts
- Dynamic graph drawing resp. layouts
- Graph layouts based on user study results
- Graph drawing aesthetics

Static graph drawing is related since our algorithm type of choice is rooted in the domain of static graph drawing. Pairwise visual comparison, in our case of DAGs, can be transferred into the domain of dynamic graph drawing. Let G_1 (base graph) and G_2 (alternative) be a pair of DAGs differing by N node and/or edge changes. Given that per time step t , starting with t_0 , N changes happen then it is $(G_1, G_2) = (G_{t_0}, G_{t_0+N})$. This relationship can be repeated for every two graphs in the set of dynamic graphs – i.e., pairwise visual comparison is basically a comparison of two graphs of the dynamic series which, consequently, makes dynamic graph drawing work related to ours. We based our layout development on the results of our previous commonalities- and difference-coined visual comparison studies (cf. Chapter ??). Consequently, other graph layouts resulting from such an approach are related. Graph drawing aesthetics are well-accepted measures for assessing the drawing quality of a layout result.

So, for sure, they also play a pivotal role for our work – i.a. because we have to ensure that our shape changes only have little influence on the already optimized graph aesthetic criteria.

1.1.1 Static Graph Layouts

There are various types of algorithms for laying out node-link diagrams. Amongst others, there are Sugiyama-like layouts (cf. e.g., [83, 24]), orthogonal layouts (cf. e.g., [29, 21]), balloon or bubble layouts (cf. e.g., [42, 22]), and radial layouts (cf. e.g., [29, 24]). However, Burch et al. [20, 19] found that Sugiyama-like layouts with the root placed on top outperforms other types such as orthogonal or radial layouts when it comes to humans working with the visualization. Sugiyama-like layouts are variants of the seminal layout algorithm of Sugiyama et al. [82]. These layout variants differ mainly in the optimization algorithm used for maximizing aesthetics – examples for edge crossing optimization are i.a. global or local sifting, median, or the barycenter method [47, 23]. Barycenter and median are easy to implement and lead to better and faster results than sifting [23]. For DAGs, in particular, edge crossing minimization and the preservation of symmetries are relevant [24, 15].

1.1.2 Dynamic Graph Layouts

While specialized layouts may be developed, a widely applied strategy is to use a static layout (see above) and extend it for the dynamic case. An important feature of the dynamic layout is the preservation of the mental map [71, 9]. It means a stable visualization where “the placement of existing nodes and edges should change as little as possible when a change is made to the graph.” [23]: Methods for ensuring stable node-link visualizations of dynamic graphs have been extensively explored (cf. i.a. [5]). In early papers on this topic, this notion has been termed the “preservation of the mental map” [31, 63]. Today, it is rather denoted as “drawing stability”. A number of possible property optimizations to achieve mental map preservation were proposed in these works. These include orthogonal ordering, topology, scaling, horizontal shuffle, and force-scan. Most of this work, and other work emerging around the same time [66], considered the scenario of a user interacting with a visualization where nodes were added/removed/re-positioned by user interactions and a balance between drawing stability and quality needed to be struck. The observance of this criterion is ensured by using so-called supergraphs for offline graph drawing. This is also applicable to our case, as we know the compared graphs in advance. In this case, a supergraph is constructed from the input graphs and then the supergraph is laid out. This can be a strict or elastic case. The strict case is also called foresighted layout without tolerance. The strict case positions all nodes at the same location across all graphs the supergraph is constructed from. It fully ensures the preservation of the mental map [25, 26].

Drawing stability has been evaluated extensively in the graph drawing literature from metric-focused [18, 81] and human-centered [9, 6, 40] experiments.

From a human-centered perspective, the benefits of a stable drawing – especially of a foresighted layout without tolerance – is in specific node and path identification, where the human can offload cognitive effort to the visualization as she knows common parts will remain in the same place during graph evolution [7]. This is also really helpful for spotting graph changes [36]. Therefore, we use a foresighted layout without tolerance.

1.1.3 Graph Drawing Aesthetics



Graph drawing aesthetics are well-accepted measures for assessing the drawing quality of a layout result. They have been mainly researched for static graph drawings. Important aesthetic criteria can be deemed to be edge crossing minimization, equal edge length, minimal node overlap, edge angle, graph symmetry, edge bending [60, 70, 68, 67, 69, 56]. These aesthetic criteria, or a subset of them, are optimized by graph layout algorithms. In our work, we build upon these works and extend them with additional drawing criteria for pairwise comparison leading to graph shape changes. We have to ensure that our shape changes only have little influence on the already optimized graph aesthetic criteria.

1.1.4 Graph Layouts based on User Study Results

Huang et al. [44] postulate the need for the consideration of human notions, perception, or cognitive processes for graph visualization since according to Huang et al. [44] “to produce truly user cognitively friendly visualizations, well-grounded cognitive theories and design guidelines are needed.” Amongst others, Kieffer et al. [50], Coleman et al. [23], Siebenhaller et al. [80], and Lin et al. [59] employed an approach where their final layout considers human notions, perception, or cognitive processes to make the graph visualization cognitively friendly for humans.

Moreover, researchers assessed with which layout users can work best (cf. e.g., [20, 57]) or how users create graph layouts (cf. e.g., [85, 28]). Specifically for hierarchic data, Burch et al. [20, 19] and Archambault et al. [8] analyzed the influence of graph layout on graph readability. They found that Sugiyama-like layouts are best readable for trees and DAGs.

1.2 Shape

In our study on visual comparisons with respect to commonalities (cf. Section ??), we found that humans are sensitive to small variations in shape. They denoted DAGs like this  as “narrow pyramids” and DAGs like this  as “wide pyramids”. Further recent studies have found the same across different visualization types: scatterplots [65], star plots [53, 54], star glyphs [37], matrix order [14], and geometric shapes for cartographic representations [52]. Here-with, we find strong substantiation of our idea to exploit the human sensitive notion of shape for improving the detectability of DAG changes in the context of pairwise visual comparisons.

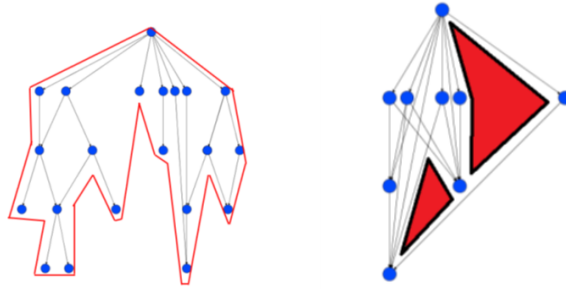


Figure 2: Shape in the graph visualization domain – outer shape (left – red line), inner shape (right – red areas). (Figure based on original Figures from [76])

As we found with our two visual comparison studies, in the context of pairwise visual comparison the factor shape consists of the outer and the inner shape of the DAG. What exactly does this mean? We would like to explain this using the doughnut and Bavarian doughnut analogy: If we asked you what the shape of a doughnut is, you would answer “A circle with a hole in the middle – something like this \odot .” If we asked you what the shape of a Bavarian doughnut is, you would answer “A circle – something like this \bigcirc .” The “circle” is the outer shape and the “hole in the middle” is the inner shape. Transported into the domain of graph visualization – the outer shape is a hull which encloses the visualized node-link diagram and the inner shape are the white space areas which result from laying out the DAGs and visualizing them as node-link diagrams (cf. Figure 2).

1.2.1 Outer Shape – Hull

A shape of visual objects is often defined using a so-called hull, contour, boundary, outline, or enclosing polyline. All are different names for the same concept of defining a visual object covering, i.e., encompassing or including, visual elements of an object [78, 88, 37]. There is a large variety of shapes for objects in 2D, in particular objects consisting of a finite set of 2D points [32]. Shapes can cover all elements, like the convex hull does, or only parts of the elements – e.g., without outliers [77]. As we are interested in changes of the DAGs’ hull we aim for shapes that enclose all elements.

The shape can have various forms, such as a bounding box, a bounding circle, a triangle, or more complex shapes such as a convex hull, a concave hull, a butterfly, or an alpha shape [78, 77, 88, 41, 33, 32]. The hull can directly bound the elements like the convex or the concave hull and the alpha shape, build so-called skeletons (e.g., MST [88]), or can be more distant from the elements, e.g., hulls using so-called distance fields [46] or the alpha-disks – shapes using centered circles [32].

The shapes may include holes or not [78]. The holes refer to ‘empty’ local

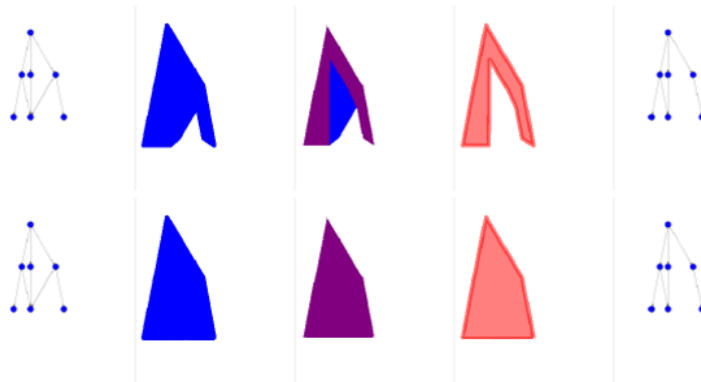


Figure 3: Example based illustration of the influence of the hull type on the shape and also the shape change of DAGs visualized as node-link diagrams.

areas, where no objects are located. These areas are fully surrounded by areas with objects, In mathematical geometry topology, they also identify objects of genus-1 or above [64]. Shapes with holes, are more general than only outer shapes – outlines [33]. An example of such a general shape is alpha-shape and its variants [32]. The local empty areas correspond to the notion of the inner white space in our work.

Often, shape refers to the outer hull of an object such as the concave or the convex hull [30]. As shown in Figure 3, the choice of the hull can have impact on the shape change of DAGs visualized as node-link diagrams. The top image shows that adding an edge to a DAG can lead to a shape change for a concave hull, but the shape remains constant for the convex hull. In other cases, an addition of one edge can change also the convex hull. Thus, the choice of the hull type has an impact on shape change. All above mentioned shape definitions refers to shapes of 2D points. However, graphs resp. DAGs include not only points (= nodes), but also connecting lines (= edges). Figure 3 shows that edges may play an important role for shape change. Related work on graph shapes (cf. e.g., [30]) focuses on large graphs where the graph shape can be approximated solely by points (= nodes). Moreover, the paper by Eades et al. [30] refers to undirected general graphs. Directed acyclic graphs laied out with a Sugiyama-like layout in 2D space have also a special top-down form, that should be considered. Owing to the variety of shape definitions and the need for graph shapes with edges, it is challenging to find a suitable shape definition for DAGs. In order to address this challenge, we conducted a qualitative user study which showed the DAGs’ shape type perceived by humans.

Qualitative User Study. We asked twenty participants to draw the outer shape of a set of DAGs. We used the same DAGs as we used for our visual comparison study with respect to commonalities and also presented the visualized DAGs as a print out. The participants should draw the shape of the DAGs with

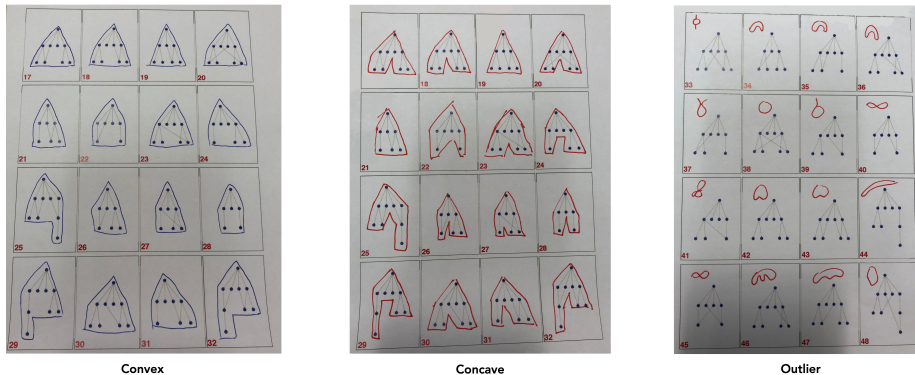


Figure 4: Qualitative user study on the shape of DAGs – examples of the hull types our participants drew. 11 out of 20 participants drew a concave hull. Six participants drew convex hulls and three participants were outliers.

a pen. We neither trained nor instructed participants on this task. As for the influence factors for the human similarity notion, we wanted to find out which shape humans see when they are asked for the outer shape of a DAG visualized as a top-rooted node-link diagram without any priming which training or instructions may cause [35, 51, 48, 3, 3].

Two coders evaluated the participants’ drawings. Both coders employed a top-down qualitative content analysis [79, 74]. This method is especially used for studying verbal material, but is also used for images [34]. It is a systematic method based on a system of categories – a coding scheme.

The result of the coders’ coding consensus was that the participants drew three types of shapes (cf. Figure 4):

- Convex hulls
- Concave hulls
- Outliers

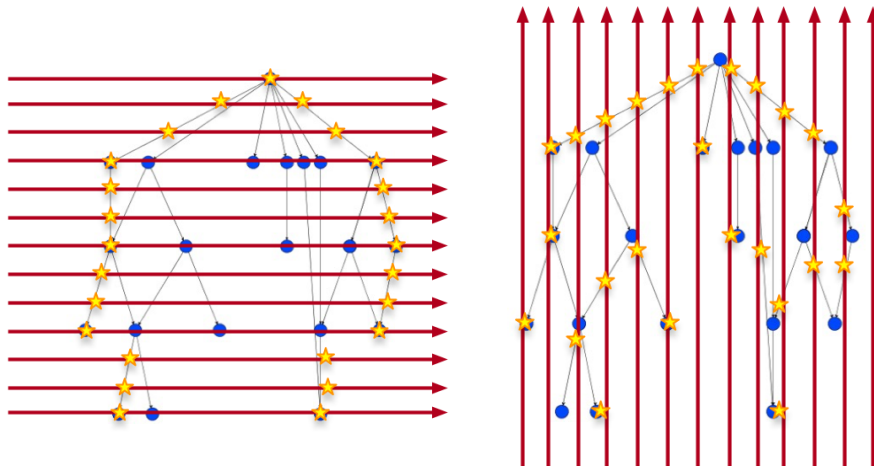
11 out of 20 participants drew a concave hull (cf. Figure 4 – **Concave**). Six participants drew convex hulls and three participants were outliers (cf. Figure 4 – **Convex**, **Outlier**). They, for instance, applied affine transformations to the visualized DAGs to achieve more complex formations like something which resembles the infinity symbol (∞). The results show a tendency for the concave hull. So, we proceed with the concave hull. But, certainly, there is still room for detailing the result – 1) how tightly the hull enclose the DAG and 2) when participants tend to draw a mixture of both a concave and a convex hull. To make our algorithm also usable when these results are clarified, we offer input parameters that allow to define the hull shape between convex and concave as well as how tightly the hull should enclose the DAG. For our calculations we tuned those parameters so that the characteristics of the resulting concave hull like

degree of enclosure and hull shape resembles the characteristics of the concave hulls drawn by our participants (degree of enclosure: 10%, hull shape – concavity: 80%). The calculation of the enclosure degree is in line with alpha-shape circles [32] and distance fields by Kalbe et al. [46].

Our Outer Shape Algorithm. Convex and concave can be seen as two extremes of a continuous space of hulls enclosing all objects of the node-link diagram with a closed polyline. The concave hull ‘cuts out’ empty space around the enclosed objects (cf. Figure 5 – (c)). These hulls are commonly calculated for 2D points. The challenge was to calculate the concave hull that is suitable for Sugiyama-like, top-rooted node-link diagrams – i.e., consider edges – and corresponds to the shapes drawn by the study participants. We developed an algorithm that calculates the hull using a ray-tracing-like approach, which takes advantage of the NLDs’ top-rootedness for sending out the rays (cf. Figure 5 – (a), (b)).

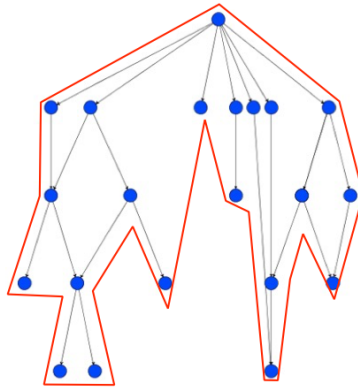
To be able to also consider edges, we approximate nodes by points and edges by sets of points. The number of points on the edge is configurable via the number of rays. Larger number of rays increases the precision, but leads to longer runtime. Horizontal and vertical parallel rays, cf. Figure 5 a), b) – red arrows, identify most-left, most-right, most-top and most-bottom nodes and edges. The intersection points of the rays and the nodes resp. edges are the points which finally form the concave hull (cf. Figure 5 a), b) – yellow stars; Figure 5 c)). The spacing of the rays determines the number and size of the concave hull’s ‘cut-outs’. According to the study, the nodes positioned in unity space¹ should not produce cut-outs, and larger spaces should produce cut-outs. Therefore, the spacing of the rays depends on the horizontal spacing parameter of nodes p_{HS} . Based on the results of our qualitative user study, we use $20 = p_{HS}/4$ points. We tried up to 80 points.

¹nodes which are positioned according to the layouts horizontal spacing parameter – in our case: $80 = p_{HS}$



(a) Horizontal rays which determine the left and the right side of the DAG's outer shape.

(b) Vertical rays which determine the bottom and the top side of the DAG's outer shape.



(c) Resulting concave hull.

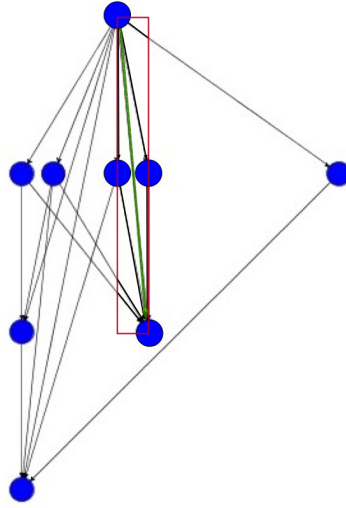
Figure 5: Outer shape algorithm – schematic representation: The intersection points of the rays and the nodes resp. edges are the points which finally form the concave hull which is shown in Figure c). (Figure based on Figures from [76])

1.2.2 Inner Shape – White Space

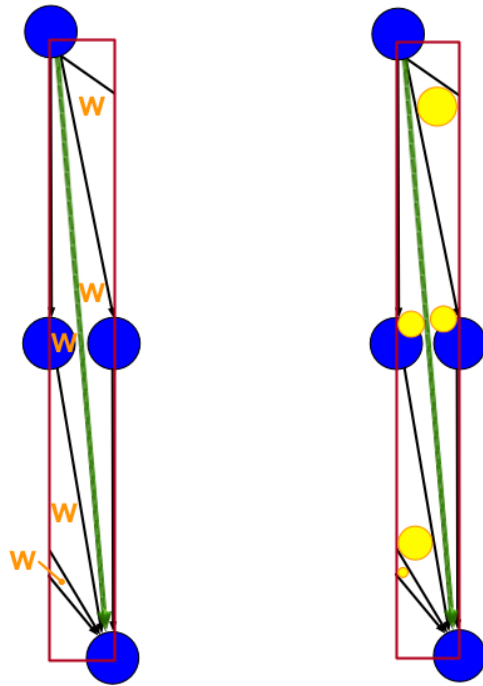
Inner shapes are holes — local areas without any elements [78, 32]. White space in node-link diagrams are local areas without nodes and without edges. They have very low local visual graph density [?]. For sets of 2D points, alpha shapes, and circular hulls [77, 32] have holes, when there are no points within a circle of a pre-set radius parameter. We extend this idea for node-link diagrams, and define white space as the area enclosed by a closed polygons of nodes and edges (cf. Figure 2 – right).

Our Inner Shape Algorithm. Our white space algorithm works within the framework of a bounding rectangle (cf. Figure 6 a) – **red rectangle**). Within this, our algorithm searches for all faces enclosed by polygons of nodes and edges. Initially, a rectangle polygon is defined that corresponds to the bounding rectangle. Now the initial polygon is divided into new polygons by each edge that intersects the rectangle (cf. Figure 6 b)). This is done until all edges that intersect the rectangle have been accounted for. For all these created polygons we calculate the largest inner circle and estimate the white space area with the circular area of the largest inner circle (cf. Figure 6 c)). Finding the center point for an arbitrary polygon is not a trivial problem. For runtime reasons, we use the algorithm of Agafonkin et al. for this calculation [2]. This is an extension of the algorithm of Garcia-Castellanos et al. [38].

If the bounding rectangle encloses a graph change, as in Figure 6, then the width of the bounding rectangle for edges is defined by the coordinates of the nodes that this edge connects. For a node change, the width of the bounding box is defined by the nodes' positions adjacent to the changing node and remaining the same.



(a) Bounding rectangle on an example DAG.



(b) Subdivision of the bounding rectangle into the polygons of nodes and edges. (c) Largest inner circles of the polygons of nodes and edges.

Figure 6: Inner shape algorithm – schematic representation. (Figure based on Figures from [76])

1.3 Our Shape Change Enhancing Hierarchical Layout Algorithm

Our shape change enhancing layout is based on a Sugiyama-like hierarchical layout from the JUNG graph drawing Library [84]. We chose a Sugiyama-like layout since Burch et al. [20, 19] found that this layout type outperforms other types such as orthogonal or radial layouts. As the layer assignment algorithm, our base implementation uses the longest path layering. The benefits of this layering algorithm are that it is linear with respect to runtime complexity and it produces DAG layouts with the minimum number of layers [83]. This avoids the hierarchical layouts to become long and thin which negatively impacts graph readability [83]. Further, it uses the barycenter method for edge crossing minimization. According to E. Mäkinen et al. [62], the barycenter method is a very good solution regarding runtime complexity and result: “The time complexities of all of these new methods are clearly bigger than that of the barycenter heuristic. Since the number of edge crossings decreased is only marginal, we prefer the barycenter heuristic.” It also optimizes the graph drawing’s visual symmetry and employs a foresighted approach with no tolerance. An increased visual symmetry improves the readability of a graph drawing [55, 69]. Purchase et al. [68] even consider visual symmetry as one of the most important graph drawing aesthetics. According to Archambault et al. [4], a strict drawing stability is in general important for the viewer’s orientation in the graph. In addition to that, we found with a further user study evaluating different layout approach ideas that an approach with tolerance creates shape changes which are likely to suggest the human viewer that the graph change is larger than the change that actually happened. Figure 7 shows an example. The top row shows the approach with tolerance and the bottom row shows the approach with no tolerance. In the top row, we can clearly see that the approach leads to a large shape change. However, it also leads to a change of shape in areas of the outer hull where no graph change happened. We believe that this is why the approach with tolerance leads to shape changes which are likely to suggest the human viewer that the graph change is larger than the change that actually happened. In the bottom row, we can see that the no tolerance approach also leads to a considerable shape change. This shape change is in the area of the outer hull where the actual graph change is located.

Our shape change enhancing layout extends this base implementation with a phase for increasing the number of outer-shape-relevant changes and a pre- and a post-processing phase (cf. Figure 8). Herewith, our layout implements the novel drawing criteria needed for enhancing the shape change:

- We need drawing criteria which lead to outwardly swapping as many graph changes as possible.
- We need drawing criteria which lead to shape changes by repositioning the outwardly swapped DAG changes.
- We need criteria which deal with DAG changes which are not possible to

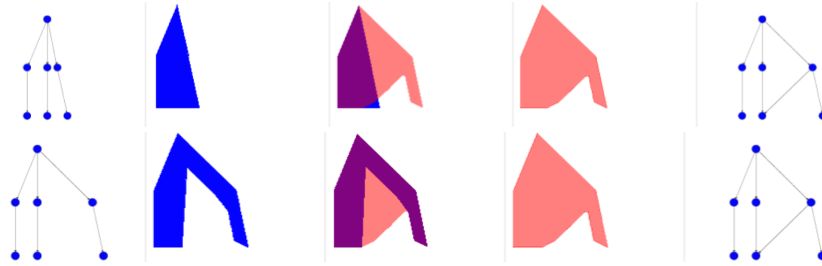


Figure 7: Shape change enhancing hierarchical layout algorithm – effects of (no) drawing stability tolerance on the outer hull: The top row shows the approach with tolerance and the bottom row shows the approach with no tolerance. In the top row, we can clearly see that the approach leads to a large shape change. However, it also leads to a change of shape in areas of the outer hull where no graph change happened. We believe that this is why the approach with tolerance leads to shape changes which are likely to suggest the human viewer that the graph change is larger than the change that actually happened. In the bottom row, we can see that the no tolerance approach also leads to a considerable shape change. This shape change is in the area of the outer hull where the actual graph change is located.

outwardly swap – nevertheless we also need a change of the DAG’s shape for those as well.

The extension-based principle was already successfully used by Diehl and his colleagues [26] to visually prepare the graph layout for changes that happened over time. This principle has two main advantages:

- it ensures that the new drawing criteria are based on the state of the art criteria and layout result since the extension happen after the Initialization phase.
- it allows to change the state of the art Sugiyama-like layout implementation from the Initialization phase since the extension happen after the Initialization phase.

1.3.1 Initialization

Our layout requires at least one one base graph and at least one alternative graph which shall be visually pairwise compared to the base graph. Throughout the initialization, we calculate for each base graph and alternative pair the supergraph. We lay out each supergraph with the afore explained base Sugiyama-like hierarchical layout and store the mental map. Laying out the supergraph with our base implementation ensures that the graph drawing is optimized with respect to the state of the art graph drawing aesthetics like minimized edge crossings or optimized visual symmetry. The following steps

work under the premiss to keep their effect on the optimized aesthetics as low as possible.

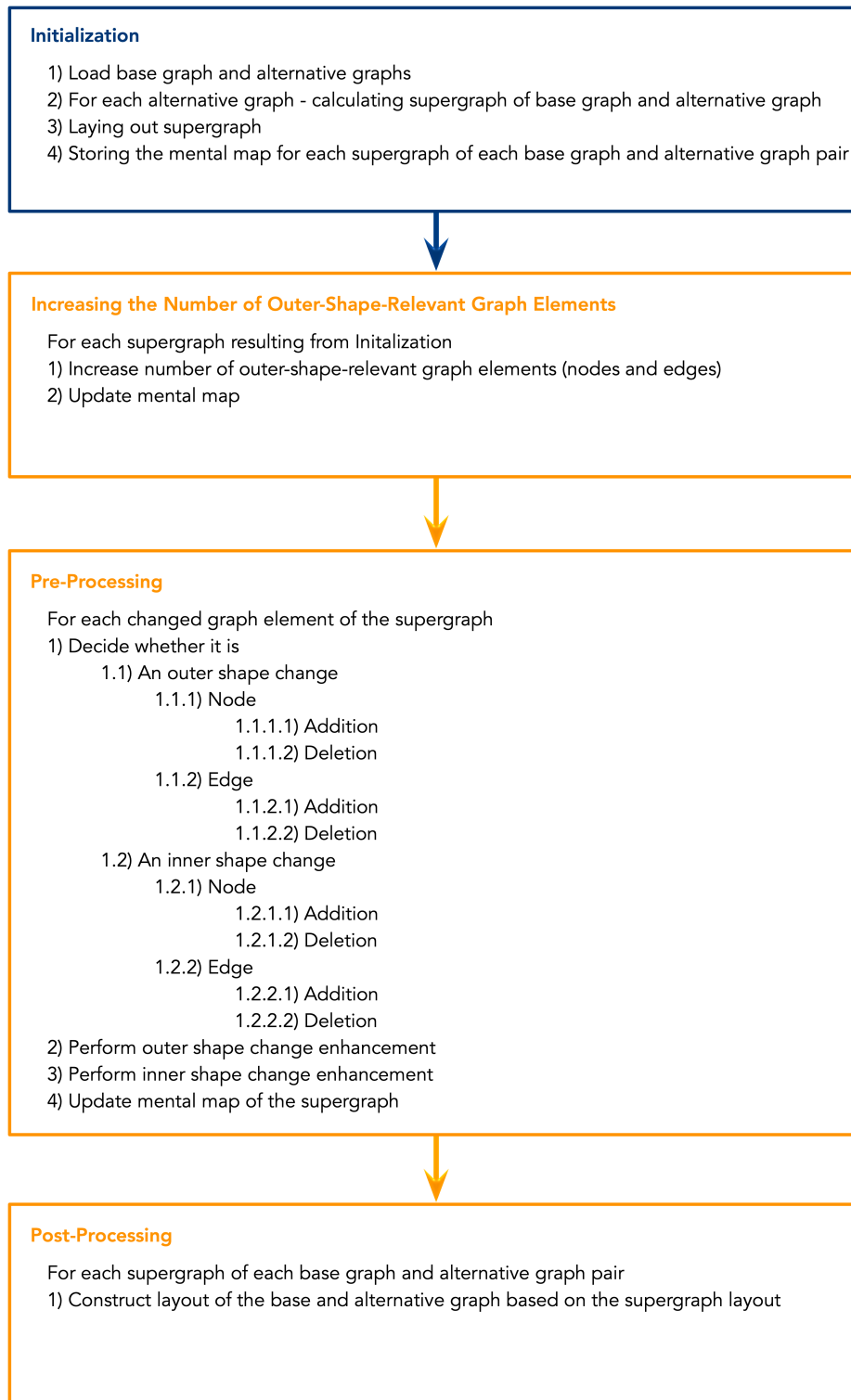
1.3.2 Increasing the Number of Outer Shape Relevant Graph Elements

The graph is examined for leaves that are not yet hull-relevant. Subsequently, a heuristic is started that builds a node chain recursively to the first graph level. The subgraph is repositioned to the left as well as to the right of the graph, as long as the aesthetics criteria are not degraded too much. Figure 9 shows a successful attempt to increase the number of hull-relevant elements.

In detail this means: First, all leaves in the graph that are not hull-relevant are identified. They are potential anchor points for the movement of a subgraph. The extension iterates the list of leaf nodes that are not hull-relevant at this point. This list must be updated after each attempt to increase the number of hull-relevant elements, since leaf nodes may also have become hull-relevant due to a move action. The method starts at the first node of the non-hull-relevant leaf node list. First, a backup of the current positions is created. This backup helps to restore the initial state should the move action negatively influence the optimized graph aesthetics criteria too much.

Recursively, the parent nodes are collected up to the first level – level below the root node. Only the first parent node is taken always. As soon as the level below the root is reached, the recursion ends. At the level below the root, all parent nodes are included in the collection list. We do this to avoid straight chains of nodes and edges. If it happens that all nodes of the first DAG level are included in the collection list, either the leftmost or the rightmost node of the first level is omitted from the collection list for the further procedure, depending on the currently tested subgraph movement direction. The reason for this and for adding only one parent node in the lower levels is that otherwise there would be no more graph elements defining whether the subgraph to be moved is to the right or to the left of the actual graph.

All collected nodes are first moved to the right of the graph. Then a new layout process starts to update the mental map and absolute positions. As long as the aesthetics criteria are not negatively affected too much, the solution is considered acceptable. The node is thus removed from the list of non-hull-relevant leaf nodes. If the solution is not acceptable – i.e. the aesthetics criteria are too strongly affected – the layout is reset to the old state and the same procedure is tested on the left side of the graph. If there is also no acceptable solution on the left side, the layout is also reset. The node is thus removed from the list of non-hull-relevant leaf nodes. The method ends when all potential nodes have been handled.



18
Figure 8: Shape change enhancing layout – schema.

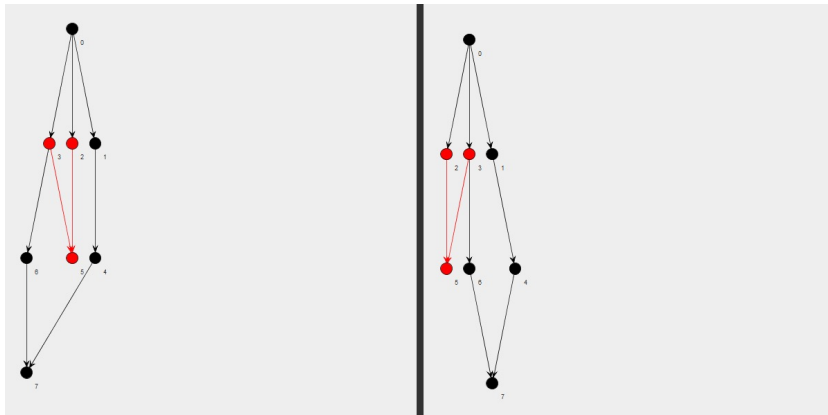


Figure 9: Increasing the number of outer shape relevant graph elements – algorithm: example of the detected subgraph which is shifted to the outer left of the example DAG. (Figure taken from [76])

1.3.3 Pre-Processing

Here, we explain the idea behind the algorithm and show the idea and algorithm results based on Figures.

Outer Shape Change Enhancement Outer shape change enhancements differentiate between nodes and edges and whether they are deleted or added to the DAG. For all adjustments, a precaution is implemented to prevent the average graph aesthetics value from being negatively affected too much. In case the aesthetics tolerance threshold (10%) is exceeded, the layout is reset to the state of the last iteration.

Node Changes. First, the nodes placed on the outside of the DAG are considered (cf. Figure 10). They are suitable for changing the outer shape of the DAG. This approach is the same for deleting and adding nodes. The new or to be deleted node is moved outwards on its horizontal axis: if it has index 0 of its layer, it is moved to the left. If it has the maximum index of its layer, it is moved to the right. This results in a larger value in the hull difference when adding or deleting a node. The displacement parameter “adaption” is configurable. After consulting our participants, we set it to the horizontal node spacing parameter (80). If a distinction is not possible because the layer has only one node, the position in relation to the whole DAG is used to decide whether the node is on the left or on the right. An iterative attempt is made to move the node further and further to the left or right until the Hausdorff distance threshold is exceeded. This is the result of a comparison of the base graph’s and the alternative graph’s concave hull. If the scalar value does not exceed the threshold, the outer shape change is considered imperceptible. In this case, the algorithm is executed again and a before-after hull comparison is performed again. This process can be limited in its number of executions by an upper bound – here set to 10. For the Hausdorff distance threshold, we again consulted our participants. The result was that the Hausdorff distance of the hulls must be greater than $\frac{30}{verticalSpacing} = \frac{30}{200}$. Furthermore, this outer shape change enhancement respects the in advanced saved mental map with respect

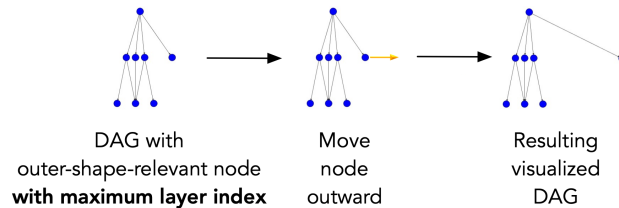


Figure 10: Outer shape change enhancement – outer-shape-relevant node changes & node has minimum or maximum layer index: schematic representation.

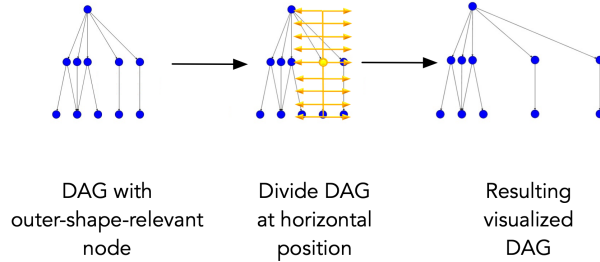


Figure 11: Outer shape change enhancement – outer-shape-relevant node changes & node does not have minimum or maximum layer index: schematic representation.

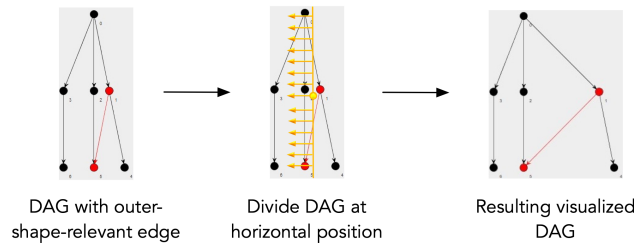


Figure 12: Outer shape change enhancement – outer-shape-relevant edge change: schematic representation.

to the nodes' relative position. After this shape change enhancement the nodes' absolute positions are updated.

The next adaptation deals with nodes that are relevant to the outer hull, but do not have the minimum or maximum position index of their layer – see Figure 11 for a schematic representation. From a conversation with a graph layout expert Prof. Dr. A. Kerren, his generalization of magnifying glass interaction with graphs gave rise to the approach of splitting the graph with a vertical axis through the node. As a result, there is an increased hull difference when the node is added or deleted. New edge intersections are also not created, since the relative positions of the nodes to each other were not changed. The graph split induces that all nodes whose horizontal position is to the left of the split center are shifted to the left. The same is true vice versa for the right side. An iterative attempt is made to move the nodes further and further to the left or right until the Hausdorff distance threshold ($\frac{30}{verticalSpacing} = \frac{30}{200}$) is exceeded. This is the result of a comparison of the base graph's and the alternative graph's concave hull. If the scalar value does not exceed the threshold, the outer shape change is considered imperceptible. In this case, the algorithm is executed again and a before-after hull comparison is performed again. This process can be limited in its number of executions by an upper bound – here set to

10. This approach is the same for deleting and adding nodes. The displacement parameter “adaption” is configurable. After consulting our participants, we set it to the horizontal node spacing parameter (80). Furthermore, this outer shape change enhancement respects the in advanced saved mental map with respect to the nodes’ relative position. After this shape change enhancement the nodes’ absolute positions are updated.

Edge Changes. There is the possibility to lengthen outer-shape-relevant edges (cf. Figure 12). In this case, the splitting method is also used. In this process, the split center is positioned at a small distance from the edge origin. It is important that the split center is placed in the direction of the edge destination. An iterative attempt is made to move the nodes left resp. right of the edge destination further and further to the left resp. right until the Hausdorff distance threshold $-\frac{30}{verticalSpacing} = \frac{30}{200}$ is exceeded. This is the result of a comparison of the base graph’s and the alternative graph’s concave hull. If the scalar value does not exceed the threshold, the outer shape change is considered imperceptible. In this case, the algorithm is executed again and a before-after hull comparison is performed again. This process can be limited in its number of executions by an upper bound – here set to 10. This approach is the same for deleting and adding nodes. The displacement parameter “adaption” is configurable. After consulting our participants, we set it to the horizontal node spacing parameter (80). Furthermore, this outer shape change enhancement respects the in advanced saved mental map with respect to the nodes’ relative position. After this shape change enhancement the nodes’ absolute positions are updated.

Inner Shape Change Enhancement For the inner shape change enhancements we employ our inner shape algorithm (cf. Section **Inner Shape -- White Space**). Here, however, we do not search all inner circles of the polygons in the bounding rectangle. We search for the polygon with the largest inner circle which is adjacent to the DAG change (cf. Figure 13). Further, we search for the polygon on the opposite site of the one with the largest inner circle which is adjacent to the DAG change (cf. Figure 13). We search for the polygon with the largest inner circle as enlarging the largest inner circle and the on the opposite side has a strong enlarging effect on the DAGs’ white space without distorting the visualized DAG entirely.

Node and Edge Changes. It depends on whether it is a node or edge change how the bounding rectangle is defined. If the bounding rectangle encloses an edge change, as in Figure 13, then the width of the bounding rectangle for edges is defined by the coordinates of the nodes that this edge connects. For a node change, the width of the bounding box is defined by the nodes’ positions adjacent to the changing node and remaining the same.

Approaches. We propose four different inner shape change enhancement approaches (WS1-WS4). Figure 14 shows a visualization of one and the same DAG pair visualized based on the four different white space enlarging approaches. Already here, in Figure 14, we can spot strength and weaknesses

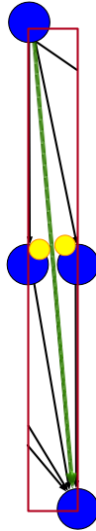


Figure 13: Inner shape change enhancement – an example of the polygons searched for the inner shape change enhancement: the polygon with the largest inner circle which is adjacent to the DAG change and the respective polygon on the opposite site of the one with the largest inner circle. In this example there are only two polygons adjacent to the change. However, there may be DAG changes where there are significantly more polygons adjacent to the DAG’s change. (Figure based on Figure from [76])

of the different approaches. For example, while the approaches WS1 and WS3 nicely enlarge the white space around the added edge, the approaches WS2 and WS4 rather lead to white space on the right next to the added edge.

WS1 – Horizontal Shift. WS1 shifts the nodes only on the horizontal layer, starting from the center of the inner circle. Nodes with a lower x-coordinate than the center of the inner circle are shifted to the left and those with a higher x-coordinate are shifted to the right. The displacement parameter “adaption” is configurable. After consulting our participants, we set this to twice the horizontal node spacing parameter. The displacement is multiplied by the factor f . It indicates how much of the actual displacement potential – displacement parameter “adaptation” – the circle receives. The smaller circle is scaled much higher because the size adjustment of both is aimed at – i.e., both circles shall be of equal size. **WS2 – Horizontal Shift & Keeping the Node Distance Ratio.** The second variant, like the first, allows only horizontal shifts. However, the nodes are moved in relation to their previous distance from the center of the inner circle, and not absolutely, as in WS1. **WS3 – Horizontal & Vertical Shift.** WS3 shifts the nodes on the horizontal and vertical layer, starting from the center of the inner circle. Nodes with a lower x-coordinate than the center of the inner circle are shifted to the left and those with a higher x-coordinate

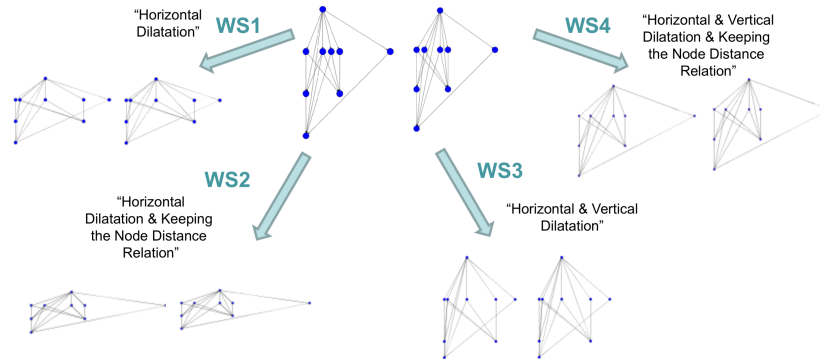


Figure 14: Inner shape change enhancement – approach variants: Already here we can spot strength and weaknesses of the different approaches. For example, while the approaches WS1 and WS3 nicely enlarge the white space around the added edge, the approaches WS2 and WS4 rather lead to white space on the right next to the added edge.

are shifted to the right. Nodes with a lower y-coordinate than the center coordinate are shifted to the top and those with a higher one are shifted to the bottom. The displacement parameter “adaption” is also configurable here. As we approximate the white space with the largest inner circle of the polygons, we have to shift the nodes on the x- and the y-axis using the same displacement parameter configuration – otherwise we would create an ellipse. Here, we also use the parameter setting of WS1. Again, the displacement is multiplied by the factor f . **WS4 – Horizontal & Vertical Shift & Keeping the Node Distance Ratio.** The fourth variant also allows horizontal and vertical shifts. However, unlike the third variant, the nodes are moved in relation to their previous distance from the center of the inner circle, and not absolutely, as in WS1 and WS3.

In all approaches, the circles are enlarged until the white space areas of the two circles exceed the white space threshold. This threshold is relative to the graph area. Consultation with our participants indicated that the white space threshold should be larger than 5% of the total graph area of the visualized DAG. We calculate the graph area based on the convex hull. Similarly, for all approaches, a precaution is implemented to prevent the average graph aesthetics value from being negatively affected too much. In case the aesthetics tolerance threshold (10%) is exceeded, the layout is reset to the state of the last iteration. Furthermore, this outer shape change enhancement respects the in advanced saved mental map with respect to the nodes’ relative position. The iterative attempt to enlarge the white space can be limited in its number of executions by an upper bound – here set to 10.

1.3.4 Post-Processing

The resulting layout applies to the supergraph. To use the layout for the base graph, the supergraph is rebuilt to resemble the base graph. The rebuilt supergraph then replaces the base graph. The supergraph is then rebuilt to match the alternative graph. This then replaces the alternative graph. This results in the layout of the alternative graph.

1.4 Evaluation

In our evaluation, we compare our shape change enhancing layout with our base implementation which we explained in Section 1.3. For our shape change enhancing layout, we evaluate our outer shape change enhancements and the different approaches we proposed for the inner shape change enhancement. For the inner ones, however, we leave out approach WS2 as it performs considerably worse than the others. Figure 14 substantiates that.

1.4.1 Dataset and Graph Changes

We randomly generated 100 base graphs with 21 nodes and 61 edges. This corresponds to realistic size and properties of for instance contagion graphs of hospital disease spread or gene mutations [89, 58]. We change the base graphs by adding/deleting one node/edge, by adding three nodes, and by adding one node and two edges. We perform those changes at all possible positions in the base graph.

We first analyze each change individually. The change types are: added node, removed node, added edge, removed edge. The advantage of the single changes is that hull-relevant changes and white space changes can be considered and evaluated in isolation without interacting with each other. The evaluation of the single change is the controlled setting to see if the chosen approach works per se. We investigate the performance of our layout for multiple simultaneous changes using the following two scenarios: added 3 nodes, added 1 node and 2 edges.

These are realistic in different contexts – explained using the hospitalization context:

- Added 3 nodes:
It may well be that three patients are hospitalized in one day.
- Added 1 node and 2 edges:
Another admitted patient is placed in a three-bed room. There are already two other patients there. It may also be that one patient is hospitalized in a single room and two pairs of patients have met at a checkup.

1.4.2 Evaluation Metrics

We employ specific metrics for the outer-shape-relevant changes and for the inner-shape-relevant changes. The graph aesthetic, we employ for both the

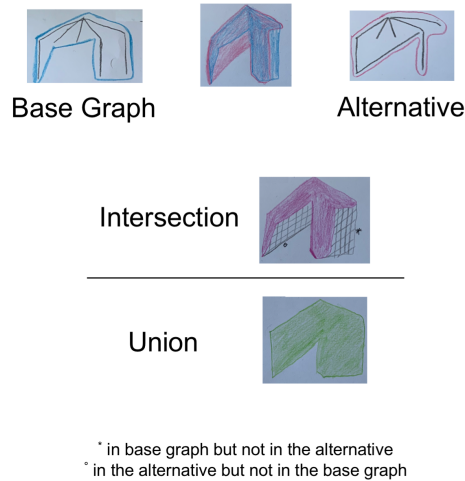


Figure 15: Shape change enhancement evaluation metric – intersection over union: schematic representation.

outer and the inner shape change enhancements since the graph aesthetics are the fundamental rules of graph drawing which ought not to be negatively impacted by both of our shape change enhancements. We also calculate the absolute difference, the ratio, and the (weighted) average for each shape change enhancement evaluation metric.

Outer Shape Change Enhancement Evaluation Metrics. Normalized Hausdorff Distance Average. As Huttenlocher et al. [45] explain, the Hausdorff distance measures the extent to which each point of [one] set lies near some point of [another] set and vice versa. Consequently, it is a good and easy and quickly to calculate approximation of how much the outer hull of two DAGs changed. For the formula and calculation details, please refer to [10]. To improve comparability, we also take the hull size into account and normalize the Hausdorff distance results by multiplying it with $\frac{1}{\text{concaveHullSize}}$. We calculate the average by summing up all the normalized Hausdorff distance results for all alternatives and dividing the sum by the number of alternatives.

Since the Hausdorff distance works with the maximum, it would only consider the maximum hull change when there are more than one DAG change which are outer-shape-relevant. In our point of view, this would be an approximation which is too rough. So, we introduce the intersection over union metric for more than one outer shape change enhancement.

The **Intersection over Union** is the average ratio of the intersection area of the concave hull of the base graph and the concave hull of the alternative graph in relation to the union area of these. An exemplary illustration is shown in Figure 15 below, where the hull of a base graph is shown on the left and the hull of an alternate graph is shown on the right. In the center, both hulls are

superimposed. There you can see the intersection area. It is the area where the blue hull of the base graph and the pink hull of the alternative graph overlap (cf. also Figure 15 – **Intersection**). The union area is the area which is covered by both hulls (cf. Figure 15 – **Union**). The intersection over union result expresses the area change in relation to the area covered in total.

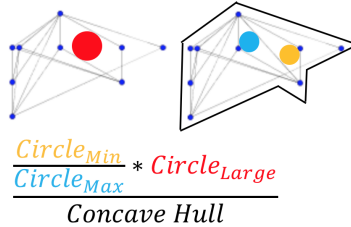


Figure 16: Schematic representation of the relative white space average evaluation metric. For each inner shape change, the resulting white space is approximated by its inner circle (**Circle_{Large}**). This is multiplied by the ratio of the two white space circles adjacent to the inner change (**Circle_{Min}**, **Circle_{Max}**). Here, the assumption is that a change is seen particularly well if the two circles adjacent to the inner change are as equal as possible. The change is then as central as possible in the white space. For comparability of the results between the graphs, the result is divided by the concave hull (**Concave Hull**).

Inner Shape Change Enhancement Evaluation Metrics. Relative White Space Average. Figure 16 shows a schematic of the formula. For each inner shape change, the resulting white space is approximated by its inner circle (cf. Figure 16 – **Circle_{Large}**). This is multiplied by the ratio of the two white space circles adjacent to the inner change – **Circle_{Min}**, **Circle_{Max}** – because the assumption is that a change is seen particularly well if the two circles adjacent to the inner change are as equal as possible. The change is then as central as possible in the white space. For comparability of the results between the graphs, the result is divided by the concave hull (Figure 16 – **Concave Hull**). We calculate the average by summing up all the relative white spaces for all alternatives and dividing the sum by the number of alternatives.

Evaluation Metrics for Both Shape Change Enhancements Aesthetic Criteria Average. For all alternative graphs, all previously defined aesthetics criteria were calculated and the average of these was formed under equal weighting. A value of 1.0 means that all alternatives in each criterion have an aesthetics value of 1.0. The aesthetics we use are those from H. Purchase [68] and Dunne et al. [27] since the current body of work on drawing quality evaluation reflects that those are amongst the most frequently used criteria – also specifically for our graph and visualization type. The aesthetics criteria of H. Purchase and Dunne et al. i.a. encompass the number of edge crossings,

angular resolution, edge bend, and symmetry. For the encompassing list and details on the aesthetics' calculation please refer to the work of H. Purchase [68] and Dunne et al. [27]. Currently, we use equal weights for all aesthetic criteria, since it is not apparent from related work which aesthetic criterion should be weighted more heavily than another. We introduced a weighting factor for each aesthetic criterion to allow a weighting when the related work does provide this information in the future or the allow the user of our layout to configure it according to her needs. The criterion is needed to calculate how high the costs of our shape change enhancements are in relation to the drawing quality which is measured by the aesthetic criteria. We calculate the average by summing up all the aesthetic criteria results for all alternatives and dividing the sum by the number of alternatives.

Absolute Difference of Our Shape Change Enhancing Layout and of the Basis Implementation. For a difference column, each is the absolute average difference between the respective computed metric for our shape change enhancing layout and for the base implementation. For example, the difference column of the average Hausdorff distance indicates the absolute average difference between the average Hausdorff distance of our layout and that of the base implementation. The difference tells the absolute average by how much better or worse our layout is.

Better, Equal, or Worse in Percent. This metric describes the percentage relative to the number of all alternatives of how often our layout was better than the base implementation, how often both were equally good, and how often our layout was worse than the base implementation. The calculation of these values is based on the absolute difference metric.

Basis Implementation Better. In cases when the base implementation outperforms our layout, the absolute difference is < 0 .

Basis Implementation = Shape Change Enhancing Layout. If both layouts are equally good, then the absolute difference is 0.

Shape Change Enhancing Layout Better. In case our layout outperforms the base implementation, the absolute difference is > 0 .

Metric Ratio. The ratio column is formed by dividing the metrics results for our layout by those for the base implementation. This results in the respective average ratio of the metric results of our layout to the results of the base implementation. The ratio of our layout to the base implementation indicates how much better or worse our layout is.

Average. When calculating the the average of a metric, each metric result is equally weighted.

Weighted Average. When calculating the weighted average of a metric, each metric result is weighted by the respective dataset proportion. The dataset proportion here is the proportion of DAGs that the respective change type produces. The change types are: added 1 node, added 1 edge, deleted 1 node, deleted 1 edge, added 3 nodes, added 1 node and 2 edges. Both type of averages indicate how the performance of the respective layout over all alternatives and change types is. So, we can gain an impression of the overall layout performance.

1.4.3 Evaluation Results

The presentation of our evaluation results is structured as follows: We first present the results of the single changes – add/delete 1 node/edge. There, we first elaborate on the results of the outer shape change enhancement evaluation and second on the inner shape change enhancement evaluation results. After that we present our results for multiple simultaneous changes. For those, we also first present the outer shape change enhancement results and then the inner shape change enhancement results.

	Hausdorff Distance Average (Base Implementation)	Hausdorff Distance Average (Shape Change Enhancing Layout)	Absolute Difference	Metric Ratio	Dataset Proportion
Add 1 Edge	0.2094	0.5842	0.3748	2.7904	0.4085
Add 1 Node	0.7097	1.1822	0.4725	1.6658	0.4478
Remove 1 Edge	0.1648	0.3920	0.2272	2.3779	0.1076
Remove 1 Node	0.6381	0.9992	0.3611	1.5659	0.0361
Equally Weighted Average	0.4305	0.7894	0.3589	2.1000	
Average Weighted by Dataset Proportion	0.4441	0.8463	0.4022	2.1982	

Table 1: Single changes – outer shape change enhancements: normalized Hausdorff distance average results.

	Base Imple- mentation Better	Base Imple- mentation = Shape Change Enhanc- ing Layout	Shape Change En- hancing Layout Better	Dataset Proportion
Add 1 Edge	0.0185	0.2904	0.6910	0.4085
Add 1 Node	0.0018	0.2134	0.7848	0.4478
Remove 1 Edge	0.0555	0.2774	0.6671	0.1076
Remove 1 Node	0.0074	0.3603	0.6324	0.0361
Equally Weighted Average	0.0208	0.2854	0.6938	
Average Weighted by Dataset Propor- tion	0.0146	0.2571	0.7283	

Table 2: Single changes – outer shape change enhancements: better, equal, or worse in percent results with respect to the Hausdorff distance average metric.

	Aesthetic Criteria Average (Base Implementation)	Aesthetic Criteria Average (Shape Change Enhancing Layout)	Aesthetic Criteria Average Absolute Difference	Aesthetic Criteria Average Metric Ratio	Edge Crossings Average (Base Implementation)	Edge Crossings Average (Shape Change Enhancing Layout)	Dataset Proportion
Add 1 Edge	0.6734	0.6319	0.0416	0.9382	171.9860	172.6732	0.4085
Add 1 Node	0.6699	0.6587	0.0111	0.9834	165.4487	165.7475	0.4478
Remove 1 Edge	0.6734	0.6487	0.0248	0.9632	160.2947	161.0764	0.1076
Remove 1 Node	0.6727	0.6677	0.0050	0.9926	139.0258	139.3432	0.0361
Equally Weighted Average	0.6724	0.6517	0.0206	0.9694	159.1888	159.7101	
Average Weighted by Dataset Proportion	0.6718	0.6470	0.0248	0.9631	166.6106	167.1207	

Table 3: Single changes – outer shape change enhancements: aesthetic criteria average and edge crossings result.

Single Changes – Outer Shape Change Enhancement Evaluation Results, Discussion, and Conclusion. Normalized Hausdorff Distance Average. For the average Hausdorff distance, it is noticeable that our shape change enhancing layout is about twice as good as the base implementation for all values (cf. Table 1). This is true for the comparison of the absolute values of the average normalized Hausdorff distance for the different change types, as well as for the absolute difference values and the ratio values. The equally weighted average and the average weighted by dataset proportion confirm the impression that can be gained from the other values. It is also noticeable that the optimization is positive especially for the edge operations (cf. Table 1 – **ratio**: 2.79 and 2.38). There, the relative ratios are particularly high compared to the base implementation. This is probably because nodes inherently produce more shape

difference.

Relative to the average weighted by the dataset proportion, the base implementation performs better than our layout in only 1.46% of all alternatives and equally well in 25.71% of all alternatives (cf. Table 2). The equal or better performance of the base implementation is due to the fact that our shape change enhancements are reset if they exceed the tolerance parameters, such as the one for the aesthetics criteria. In 72.83% of all alternatives our layout outperforms the base implementation (cf. Table 2).

Aesthetic Criteria Average. The evaluation of the aesthetics criteria average and specifically the number of edge crossings – see Table 3 – reveals: According to the weighted average by dataset proportion, our shape change enhancements produce a loss of a mere 3.70% in the aesthetics criteria average. This is a very good result for the rather intensive interventions performed by our shape change enhancements and the increase in the number of outer-shape-relevant graph elements. We set the parameter to 10% allowed loss for the aesthetic criteria average. Looking at the individual losses, we clearly see that the 10% average is far from being reached – add 1 edge: 6.18%; add 1 node: 1.66%; delete 1 edge: 3.68%, add 1 node: 0.74%. Edges tend to have a higher impact on the aesthetics criteria, as edges have an impact on edge crossings, edge angles, edge length, and more. Looking specifically at edge crossings, we can see that our layout only produces about 0.5 more edge crossings on average than the base implementation for the outer shape change enhancements. So this is a negligible increase in edge crossings.

Conclusion. Our layout convinces with its outer shape change enhancements. It outperforms the base implementation in 72.83% of all alternatives and the cost in terms of aesthetics criteria is only 3.70%. This shows that the optimization functions achieve their goal.

	Relative White Space Average (Base Implementation)	Relative White Space Average (Shape Change Enhancing Layout)	Absolute Difference	Metric Ratio	Dataset Proportion
Add 1 Edge (WS1)	0.0016	0.0054	0.0038	3.3082	0.6178
Add 1 Edge (WS3)	0.0017	0.0065	0.0048	3.9108	0.6238
Add 1 Edge (WS4)	0.0017	0.0019	0.0003	1.1721	0.6166
Add 1 Node (WS1)	0.0015	0.0034	0.0019	2.2296	0.0278
Add 1 Node (WS3)	0.0021	0.0024	0.0003	1.1566	0.0191
Add 1 Node (WS4)	0.0017	0.0016	-0.0001	0.9234	0.0209
Remove 1 Edge (WS1)	0.0016	0.0032	0.0015	1.9449	0.3542
Remove 1 Edge (WS3)	0.0017	0.0044	0.0027	2.6279	0.3568
Remove 1 Edge (WS4)	0.0017	0.0020	0.0003	1.1833	0.3625
Remove 1 Node (WS1)	0.0001	0.0001	-0.00001	0.9107	0.0001
Remove 1 Node (WS3)	0.0001	0.0007	0.0006	7.2210	0.0003
Remove 1 Node (WS4)	0.0000	0.0000	0.0000	1.0000	0.000001
Eq. Weighted Avg. (WS1)	0.0012	0.0030	0.0018	1.0984	
Eq. Weighted Avg. (WS3)	0.0014	0.0035	0.0021	3.7290	
Eq. Weighted Avg. (WS4)	0.0013	0.0014	0.0021	1.0697	
Avg. Weighted by Dataset Prop. (WS1)	0.0016	0.0046	0.0029	2.7949	
Avg. Weighted by Dataset Prop. (WS3)	0.0017	0.0057	0.0040	3.4015	
Avg. Weighted by Dataset Prop. (WS4)	0.0017	0.0019	0.0003	1.1710	

Table 4: Single changes – inner shape change enhancements: relative white space average results.

	Base Imple- mentation Better	Base Imple- mentation = Shape Change Enhanc- ing Layout	Shape Change En- hancing Layout Better	Dataset Proportion
Add 1 Edge (WS1)	0.3291	0.0315	0.6394	0.6178
Add 1 Edge (WS3)	0.2991	0.0692	0.6318	0.6238
Add 1 Edge (WS4)	0.3674	0.0587	0.5740	0.6166
Add 1 Node (WS1)	0.4321	0.0309	0.5340	0.0278
Add 1 Node (WS3)	0.5683	0.0573	0.3744	0.0191
Add 1 Node (WS4)	0.5061	0.1020	0.3918	0.0209
Remove 1 Edge (WS1)	0.4418	0.0332	0.5251	0.3542
Remove 1 Edge (WS3)	0.3027	0.0779	0.6194	0.3568
Remove 1 Edge (WS4)	0.3290	0.0575	0.6132	0.3625
Remove 1 Node (WS1)	1.0000	0.0000	0.0000	0.0001
Remove 1 Node (WS3)	0.2500	0.0000	0.7500	0.0003
Remove 1 Node (WS4)	0.0000	1.0000	0.0000	0.000001
Eq. Weighted Avg. (WS1)	0.5507	0.0239	0.4246	
Eq. Weighted Avg. (WS3)	0.3550	0.0511	0.5939	
Eq. Weighted Avg. (WS4)	0.3006	0.3046	0.3947	
Avg. Weighted by Dataset Prop. (WS1)	0.3720	0.0321	0.5959	
Avg. Weighted by Dataset Prop. (WS3)	0.3055	0.0720	0.6225	
Avg. Weighted by Dataset Prop. (WS4)	0.3563	0.0593	0.5843	

Table 5: Single changes – inner shape change enhancements: better, equal, or worse in percent results with respect to the relative white space average metric.

	Aesthetic Criteria Avg. (Base Implementation)	Aesthetic Criteria Avg. (SCE Layout)	Aesthetic Criteria Avg. (Absolute Difference)	Aesthetic Criteria Avg. (Metric Ratio)	Edge Crossings Avg. (Base Implementation)	Edge Crossings Avg. (Shape Change Enhancing (SCE) Layout)	Dataset Proportion
Add 1 Edge (WS1)	0.6763	0.6373	0.0390	0.9424	173.1443	181.3176	0.6178
Add 1 Edge (WS3)	0.6750	0.6349	0.0400	0.9408	172.3088	181.3227	0.6238
Add 1 Edge (WS4)	0.6753	0.6401	0.0353	0.9478	171.9943	172.3701	0.6166
Add 1 Node (WS1)	0.6671	0.6195	0.0476	0.9286	173.1667	176.1296	0.0278
Add 1 Node (WS3)	0.6669	0.6208	0.0460	0.9310	176.6696	181.0352	0.0191
Add 1 Node (WS4)	0.6638	0.6291	0.0347	0.9478	176.0041	176.4449	0.0209
Remove 1 Edge (WS1)	0.6727	0.6306	0.0421	0.9374	156.9583	162.6132	0.3542
Remove 1 Edge (WS3)	0.6754	0.6333	0.0421	0.9377	157.4276	164.8217	0.3568
Remove 1 Edge (WS4)	0.6752	0.6403	0.0349	0.9483	157.1276	157.3821	0.3625
Remove 1 Node (WS1)	0.6809	0.6067	0.0742	0.8911	138.5000	150.5000	0.0001
Remove 1 Node (WS3)	0.6435	0.5919	0.0517	0.9197	132.2500	139.0000	0.0003
Remove 1 Node (WS4)	0.6836	0.6839	0.0000	1.0004	124.0000	124.0000	0.000001
Eq. Weighted Avg. (WS1)	0.6743	0.6235	0.0507	0.9249	160.4423	167.6401	
Eq. Weighted Avg. (WS3)	0.6652	0.6202	0.0450	0.9323	159.6640	166.5449	
Eq. Weighted Avg. (WS4)	0.6745	0.6483	0.0262	0.9611	157.2815	157.5493	
Avg. Weighted by Dataset (DS) Prop. (WS1)	0.6748	0.6344	0.0403	0.9402	167.4058	174.5428	
Avg. Weighted by DS Prop. (WS3)	0.6750	0.6341	0.0409	0.9394	167.0694	175.4157	
Avg. Weighted by DS Prop. (WS4)	0.6750	0.6399	0.0351	0.0480	166.6849	167.0181	

Table 6: Single changes – inner shape change enhancements: aesthetic criteria average and edge crossings result.

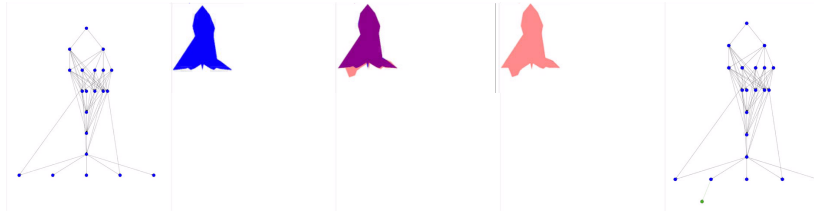
Single Changes – Inner Shape Change Enhancement Evaluation Results, Discussion, and Conclusion. Relative White Space Average.

WS1 achieves relatively, weighted according to dataset proportion, a 2.80-fold higher value than the base implementation (cf. Table 4). Leading is the WS3 approach with a factor of 3.40 – i.e., WS3 produces white spaces that are 3.40 times as large as those of the base implementation. The worst performing approach is WS4. It generates white spaces that are only 1.17 times larger than those of the base implementation. As for the inner shape change enhancements, slightly more shape change enhancements are reset, because the base implementation performs better than our layout in about 30% of all alternatives (cf. Table 5). Both are equally good in 3 – 7% of all alternatives. In about 60% of all alternatives, our layout performs better than the base implementation.

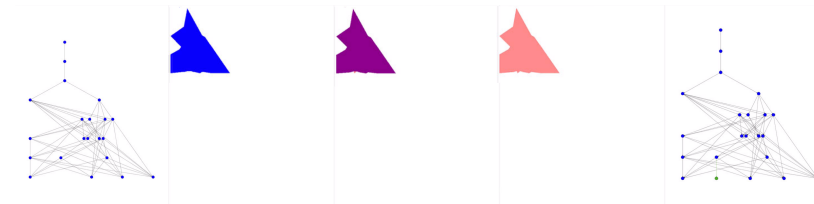
Aesthetic Criteria Average. According to the weighted average by dataset proportion of the aesthetics criteria, the WS4 approach is the best with a loss of about 5.20% (cf. Table 6). However, this approach also achieves the worst results in terms of white space enlargement. It leads to an enlargement of only 1.17. Since it preserves the horizontal and vertical node distance ratios, it leads to fewer new edge crossings, see Figure 14. However, keeping the distance ratios also leads WS4 to achieve the worst result in white space enlargement around the graph change. Furthermore, we can state that the approach WS1, which performs second best in terms of white space enlargement, leads to only 0.78% more loss than WS4 (cf. Table 6). WS3 again follows close behind with a loss of 6.06% (cf. Table 6). The inner shape change enhancements result in about twice the loss in aesthetic criteria average compared to the outer shape change enhancements. This is still a very good result, as it is still well below the tolerance parameter of 10%. Furthermore, the inner shape change enhancements tend to be even more intensive interventions to the graph layout, since more graph elements have to be moved to create white space. Thus, the larger loss can be explained by this. As far as edge crossings are concerned, WS4 is the best (cf. Table 6). It leads to 0.33 more edge crossings than the base implementation. However, as discussed earlier for the aesthetic criteria average, WS4 creates the least white space enlargement. WS1 and WS3 – the approaches that do not retain the node distance ratios – create 7.13 and 8.35 more edge crossings according to the dataset proportion weighted average (cf. Table 6). The approaches that do not keep the distance ratios tend to generate more e.g. new edge crossings. This is already evident in Figure 14. This tendency can be explained by the fact that some parts of the DAG are shifted more than others. With the underlying graph size, however, this is still a really good result which, in combination with the aesthetic criteria average and the relative white space average, allows the conclusion that, also for the inner shape change enhancements, the optimizations and the tolerance parameters fulfill their purpose.

Conclusion. Our layout can also convince with its results for the inner shape change enhancements: In about 60% of all alternatives our layout outperforms the base implementation. The cost in terms of the aesthetics criteria is 6.1% in the worst case while the allowed loss is 10%. This shows that the optimization functions achieve their goal.

Example 1 – Add 1 Node



Example 2 – Add 1 Node



Example 3 – Add 1 Node

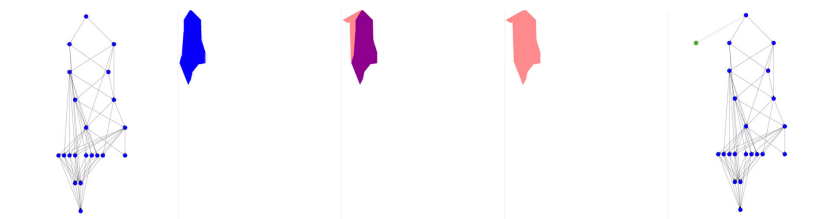
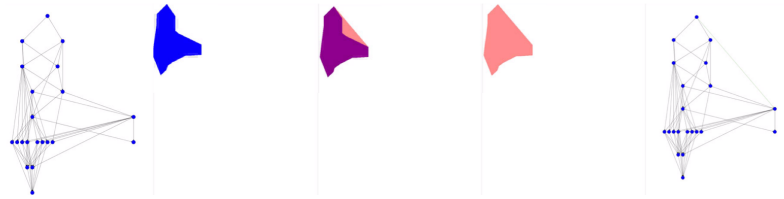
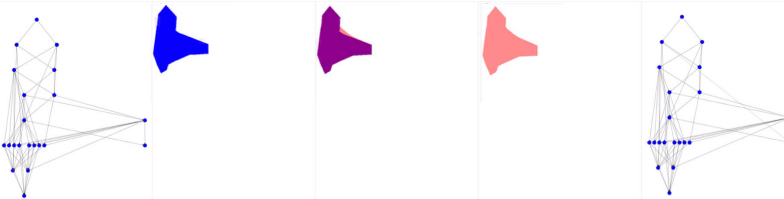


Figure 17: Single graph changes – example visualization results for single node changes and outer shape change enhancements.

Example 1 – Add 1 Edge



Example 2 – Add 1 Edge



Example 3 – Add 1 Edge

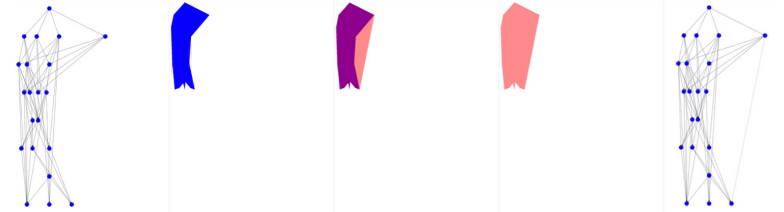
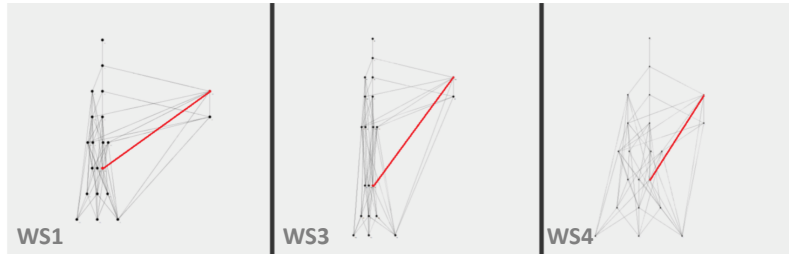
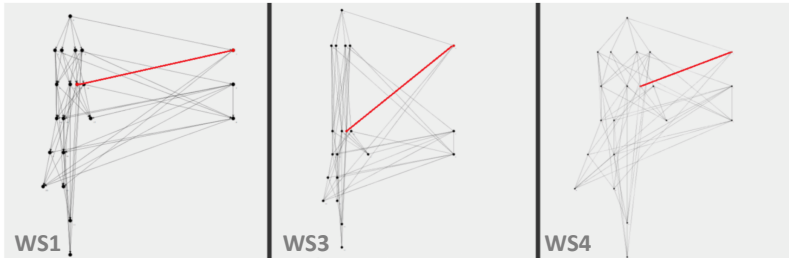


Figure 18: Single graph changes – example visualization results for single edge changes and outer shape change enhancements.

Example 1 – Add 1 Edge



Example 2 – Add 1 Edge



Example 3 – Add 1 Edge

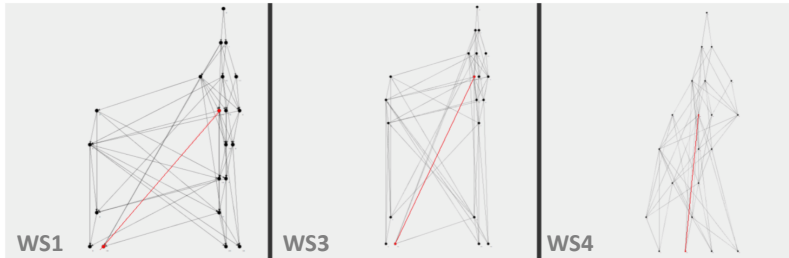
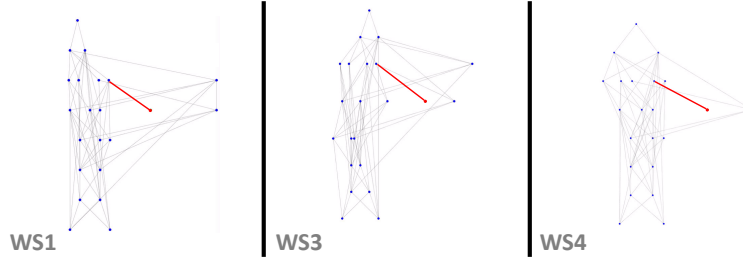
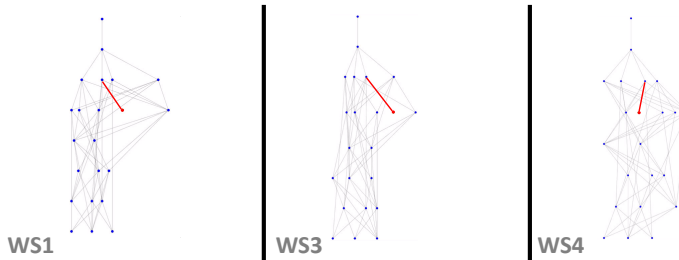


Figure 19: Single graph changes – example visualization results for single edge changes and inner shape change enhancements.

Example 1 – Add 1 Node



Example 2 – Add 1 Node



Example 3 – Add 1 Node

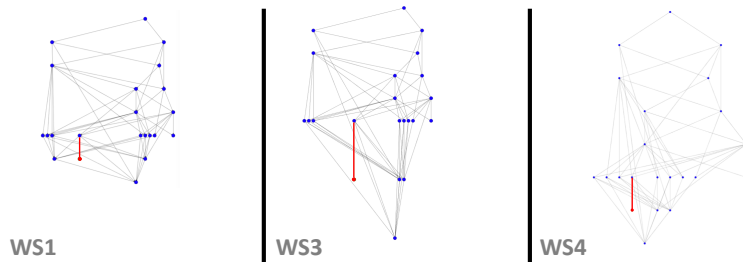


Figure 20: Single graph changes – example visualization results for single node changes and inner shape change enhancements.

Single Changes – Example Visualization Results. Outer Shape Change Enhancements. Figure 17 shows three visualization results for outer shape change enhancements for adding a node as an example. Example 1 shows the case where the new node is the only node in a layer. Since the node generates more outer hull change when moved to the left compared to the whole graph, the algorithm chooses this option. This is also the reason why the node is not

placed directly below its parent node, as is actually typical. Example 2 shows the case where the shape relevant node does not have the minimum or maximum index of a level. This splitting of the graph is similar to the inner shape change enhancements, as it is also based on moving parts of the graph. In this example, the graph split provides a relatively small change to the outer hull, which is due to the path of the edges that are around the new node – not the optimization itself. The visualized graph shows well that the optimization itself works well. The part of the graph to the left of the new node and the part of the graph to the right of the new node have been moved to the left and to the right, respectively, as desired. Example 3 shows how the outer hull was noticeably changed by an added node that was rotated outward and moved to the left. For the addition of an edge, the same picture is obtained. The optimizations work (cf. Figure 18 – **Example 1-3**). But as example 1 and 2 clearly show the then resulting change of the outer hull also depends noticeably on the course of the added edge, as well as the further edges. Example 3 shows how a full outer edge in combination with our optimization for shape relevant edges leads to a significant change of the outer hull of the graph (cf. Figure 18 – **Example 3**). Thus, the visualization examples for outer shape change enhancements support the previous evaluation results.

Inner Shape Change Enhancements. The three examples, each with an edge added (cf. Figure 19), clearly show the better performance of the white space approaches that do not respect the horizontal and vertical node distance ratio. WS1 and WS3 reliably generate white space around the graph changes, which then helps to better detect the inner graph change. WS4 confirms the impression already outlined by Figure 14. WS4 enlarges white spaces. But usually not directly at the change where the white space is supposed to be enlarged, but, due to maintaining the distance relation, the white space, which is already larger, is further enlarged. If this is not by chance, as in example 2, the white space that is at the change, another white space area is enlarged, but this one does not contain any change. For adding single nodes, cf. Figure 20, the same pattern emerges. The white space approaches WS1 and WS3 reliably create enlarged white space around the inner graph change while the WS4 approach again tends to increase white spaces that are already larger. If the already larger white space does not happen to be at the change, as in example 2, another white space area is enlarged that does not contain a change.

Conclusion. In graph drawing one always tries to draw the graphs as symmetrical as possible, because it is well known that people find symmetrical visualizations pleasant or even beautiful [72]. But as it becomes clear here, for the enlargement of certain white spaces – here: the white spaces at the graph changes – a certain asymmetry is necessary; i.e. the non-compliance with the horizontal and vertical node distance ratio. WS1 and WS3 generate white space enlargements around graph changes much more reliably, but, for example, the level distances are no longer uniform across all hierarchical levels of the graph (WS3) (cf. Figure 14). This is a certain break in the drawing symmetry of the graph. The same is to be noted for the outer shape change enhancements. Also the graph splitting and the left/right moving of nodes cause a certain asymmetry

and therefore a certain break of the drawing symmetry.

	Intersection over Union (Base Implementation)	Intersection over Union (Shape Change Enhancing Layout)	Absolute Difference	Metric Ratio	Dataset Proportion
Add 3 Nodes (WS1)	0.1325	0.2688	0.1363	2.0284	0.5965
Add 3 Nodes (WS3)	0.1394	0.2832	0.1438	2.0313	0.5967
Add 3 Nodes (WS4)	0.1394	0.2940	0.1545	2.1086	0.5967
Add 1 Node, Add 2 Edges (WS1)	0.0584	0.0828	0.0244	1.4170	0.4035
Add 1 Node, Add 2 Edges (WS3)	0.0575	0.0810	0.0236	1.4098	0.4033
Add 1 Node, Add 2 Edges (WS4)	0.0590	0.1437	0.0847	2.4372	0.4033
Eq. Weighted Avg. (WS1)	0.0955	0.1758	0.0803	1.7227	
Eq. Weighted Avg. (WS3)	0.0985	0.1821	0.0837	1.7295	
Eq. Weighted Avg. (WS4)	0.0992	0.2188	0.1196	2.2729	
Avg. Weighted by Dataset Prop. (WS1)	0.1026	0.1937	0.0911	1.7817	
Avg. Weighted by Dataset Prop. (WS3)	0.1064	0.2017	0.0953	1.7806	
Avg. Weighted by Dataset Prop. (WS4)	0.1070	0.2334	0.1264	2.2411	

Table 7: Multiple simultaneous changes – outer shape change enhancements: intersection over union results.

	Base Implementation Better	Base Implementation = Shape Change Enhancing Layout	Shape Change Enhancing Layout Better	Dataset Proportion
Add 3 Nodes (WS1)	0.0097	0.0147	0.9755	0.5965
Add 3 Nodes (WS3)	0.0138	0.0095	0.9767	0.5967
Add 3 Nodes (WS4)	0.0051	0.0119	0.9831	0.5967
Add 1 Node, Add 2 Edges (WS1)	0.0361	0.1095	0.8544	0.4035
Add 1 Node, Add 2 Edges (WS3)	0.1405	0.1167	0.7428	0.4033
Add 1 Node, Add 2 Edges (WS4)	0.0299	0.1046	0.8655	0.4033
Eq. Weighted Avg. (WS1)	0.0229	0.0621	0.9149	
Eq. Weighted Avg. (WS3)	0.0772	0.0631	0.8597	
Eq. Weighted Avg. (WS4)	0.0175	0.0583	0.9243	
Avg. Weighted by Dataset Prop. (WS1)	0.0203	0.0530	0.9266	
Avg. Weighted by Dataset Prop. (WS3)	0.0649	0.0527	0.8823	
Avg. Weighted by Dataset Prop. (WS4)	0.0151	0.0493	0.9356	

Table 8: Multiple simultaneous changes – outer shape change enhancements: better, equal, or worse in percent results with respect to the intersection over union metric.

	Relative White Space Average (Base Implementation)	Relative White Space Average (Shape Change Enhancing Layout)	Absolute Difference	Metric Ratio	Dataset Proportion
Add 3 Nodes (WS1)	0.0020	0.0042	0.0018	2.0417	0.5965
Add 3 Nodes (WS3)	0.0018	0.0043	0.0022	2.3533	0.5967
Add 3 Nodes (WS4)	0.0019	0.0018	0.000001	0.9482	0.5967
Add 1 Node, Add 2 Edges (WS1)	0.0013	0.0051	0.0035	3.8308	0.4035
Add 1 Node, Add 2 Edges (WS3)	0.0013	0.0061	0.0044	4.6106	0.4033
Add 1 Node, Add 2 Edges (WS4)	0.0014	0.0016	0.0002	1.1944	0.4033
Eq. Weighted Avg. (WS1)	0.0017	0.0046	0.0026	2.9362	
Eq. Weighted Avg. (WS3)	0.0016	0.0052	0.0033	3.4819	
Eq. Weighted Avg. (WS4)	0.0016	0.0017	0.0001	1.0713	
Avg. Weighted by Dataset Prop. (WS1)	0.0018	0.0045	0.0025	2.7636	
Avg. Weighted by Dataset Prop. (WS3)	0.0016	0.0050	0.0030	3.2637	
Avg. Weighted by Dataset Prop. (WS4)	0.0017	0.0017	0.0001	1.0475	

Table 9: Multiple simultaneous changes – inner shape change enhancements: relative white space average results.

	Base Imple- mentation Better	Base Imple- mentation = Shape Change Enhanc- ing Layout	Shape Change En- hancing Layout Better	Dataset Proportion
Add 3 Nodes (WS1)	0.4244	0.0009	0.5746	0.5965
Add 3 Nodes (WS3)	0.4572	0.0034	0.5394	0.5967
Add 3 Nodes (WS4)	0.5577	0.0064	0.4360	0.5967
Add 1 Node, Add 2 Edges (WS1)	0.2933	0.0043	0.7025	0.4035
Add 1 Node, Add 2 Edges (WS3)	0.3161	0.0239	0.6600	0.4033
Add 1 Node, Add 2 Edges (WS4)	0.4202	0.0116	0.5682	0.4033
Eq. Weighted Avg. (WS1)	0.3589	0.0026	0.6385	
Eq. Weighted Avg. (WS3)	0.3866	0.0137	0.5997	
Eq. Weighted Avg. (WS4)	0.4890	0.0090	0.5021	
Avg. Weighted by Dataset Prop. (WS1)	0.3715	0.0023	0.6262	
Avg. Weighted by Dataset Prop. (WS3)	0.4002	0.0117	0.5881	
Avg. Weighted by Dataset Prop. (WS4)	0.5022	0.0085	0.4893	

Table 10: Multiple simultaneous changes – inner shape change enhancements: better, equal, or worse in percent results with respect to the relative white space average metric.

	Aesthetic Criteria Average (Base Implementation)	Aesthetic Criteria Average (Shape Changing Layout)	Aesthetic Criteria Average Absolute Difference	Aesthetic Criteria Average Metric Ratio	Edge Crossings Average (Base Implementation)	Edge Crossings Average (Shape Changing Layout)	Dataset Proportion
Add 3 Nodes (WS1)	0.6768	0.6304	0.0464	0.9315	153.8489	154.5513	0.5965
Add 3 Nodes (WS3)	0.6768	0.6304	0.0464	0.9315	153.4370	154.7107	0.5967
Add 3 Nodes (WS4)	0.6776	0.6349	0.0427	0.9369	153.0312	153.5835	0.5967
Add 1 Node, Add 2 Edges (WS1)	0.6939	0.6436	0.0494	0.9288	136.8921	142.0985	0.4035
Add 1 Node, Add 2 Edges (WS3)	0.6934	0.6371	0.0564	0.9187	136.8641	141.9567	0.4033
Add 1 Node, Add 2 Edges (WS4)	0.6933	0.6330	0.0603	0.9131	137.2090	136.8804	0.4033
Eq. Weighted Avg. (WS1)	0.6849	0.6370	0.0479	0.9301	145.3705	148.3249	
Eq. Weighted Avg. (WS3)	0.6851	0.6337	0.0514	0.9251	145.1505	148.3337	
Eq. Weighted Avg. (WS4)	0.6854	0.6339	0.0515	0.9250	145.1201	145.2320	
Avg. Weighted by Dataset Prop. (WS1)	0.6833	0.6357	0.0476	0.9304	147.0070	149.5268	
Avg. Weighted by Dataset Prop. (WS3)	0.6835	0.6331	0.0504	0.9263	146.7526	149.5666	
Avg. Weighted by Dataset Prop. (WS4)	0.6839	0.6341	0.0498	0.9273	146.6504	146.8475	

Table 11: Multiple simultaneous changes: aesthetic criteria average and edge crossings result.

Multiple Simultaneous Changes Outer Shape Change Enhancement Evaluation Results. *Intersection over Union.* For multiple graph changes, using the white space approaches WS1 and WS3, the outer hull changes by 1.78 times compared to the base implementation (cf. Table 7). If the white space approach WS4 is used, the outer hull changes even by 2.24-fold compared to the base implementation (cf. Table 7). However, here again comes the problem that by maintaining the distance ratios, the WS4 method further enlarges white spaces that are already larger, and thus the white spaces that contain a change are not necessarily the ones that are conspicuously enlarged – unless the change happens to be in the white space that is already larger and is further enlarged by WS4. We can state that our shape change enhancing layout performs about two times better than the base implementation for multiple simultaneous changes according to the weighted average by dataset proportion (cf. Table 7). The other evaluations – equal-weighted average, average per changes, and white space method – also paint a similar picture. Comparing the proportions of how often our shape change enhancing layout achieves a better result than the base implementation shows that when the white space approaches WS1 and WS3 are used, our shape change enhancing layout achieves a better result than the base implementation in 73.70% and 75.51% of the cases, respectively (cf. Table 8). If the WS 4 approach is used, our shape change enhancing layout even achieves a better result than the building implementation in 89.93% of the cases. However, it must be emphasized again that the WS4 approach does not increase the desired white space. This of course relativizes the apparently good performance using WS4 again.

Inner Shape Change Enhancement Evaluation Results. *Relative White Space Average.* Relative to the base implementation, our WS3 approach again achieves the best result. WS3 achieves a relative white space 3.26 times as large as that of the base implementation (cf. Table 9). Our approach WS1 also achieves an excellent result with an average of 2.76 times as large relative white space (cf. Table 9). Compared to the base implementation, our approach WS4 achieves on average only a slightly better result than the base implementation itself. WS4 achieves on average a 1.04 larger relative white space than the base implementation (cf. Table 9). The results are nearly identical to the inner shape change enhancement results for single changes. Our approach WS1 and WS3 are better than the base implementation in more than and just about 60% of the cases, respectively, in the by dataset proportion weighted average (cf. Table 10). For the WS4 approach, it is more of a coincidence whether it or the base implementation is better: WS4 is better than the base implementation in 48.92% of the cases and the base implementation is better than our WS4 approach in 50.22% of the cases (cf. Table 10). In conclusion, also this metric supports the previous evaluation results.

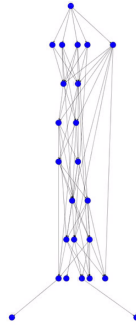
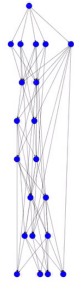
Aesthetic Criteria Average. As Table 11 shows, for multiple simultaneous graph changes, all three white space approaches have similar costs in terms of aesthetic criteria average. All three approaches result in a loss of about 7%. Given the nevertheless very strong interventions – outer and inner shape change enhancements – this is a very good result in combination with the shape-relevant

adaptations. The results of the multiple simultaneous graph changes for the achieved aesthetic criteria average are comparable to the aesthetic criteria average for the inner shape change enhancements of the single changes. That means the inner shape change enhancements have a stronger influence on the aesthetic criteria average than the outer shape change enhancements (approx. twice (cf. Sections `Single Changes - Inner Shape Change Enhancement Evaluation Results, Discussion, and Conclusion - Aesthetic Criteria Average` and `Single Changes - Outer Shape Change Enhancement Evaluation Results, Discussion, and Conclusion - Aesthetic Criteria Average`)), but the influence of the inner shape change enhancements does not become noticeably stronger as the number of graph changes increases. As far as edge crossings are concerned, WS4 is the best (cf. Table 11). It leads to 0.20 more edge crossings than the base implementation. However, as already discussed, WS4 creates the least white space enlargement. WS1 and WS3 create 2.52 and 2.81 more edge crossings according to the average weighted by dataset proportion (cf. Table 11). The approaches that do not keep the distance ratios tend to generate more e.g. new edge crossings. This is already evident in Figure 14. This tendency can be explained by the fact that some parts of the DAG are shifted more than others. With the underlying graph size, however, this is still a really good result which, in combination with the aesthetic criteria average, the intersection over union results, and the relative white space average, allows the conclusion that, also for multiple graph changes, the optimizations and the tolerance parameters fulfill their purpose.

Conclusion. Also for multiple, simultaneously occurring graph changes our shape change enhancing layout achieves convincing results: It outperforms the base implementation in about 75% of all cases when it comes to the intersection over union metric. For the relative white space average metric, our layout outperforms the base implementation in about 60% of all alternatives. The cost in terms of the aesthetics criteria are approximately 7%. This shows that the optimization functions achieve their goal.

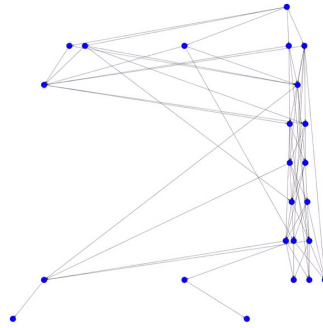
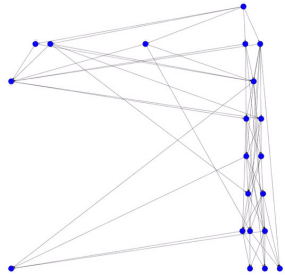
Multiple Simultaneous Changes – Example Visualization Results Also the visualization results of multiple simultaneous changes are in line with the afore discussed evaluation results. They show the afore discussed advantages and issues which were already apparent in the visualizations of single graph changes.

Example 1 – Add 3 Node

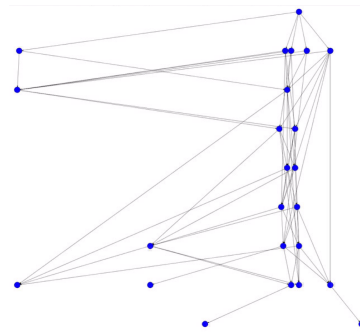
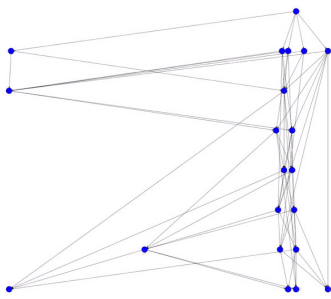


WS1
Base
Graph
1

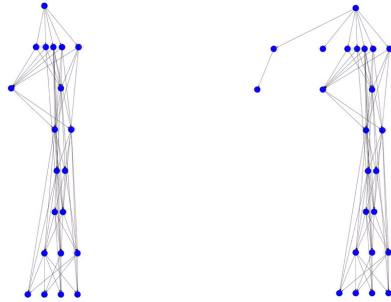
Example 2 – Add 3 Node



Example 3 – Add 3 Node

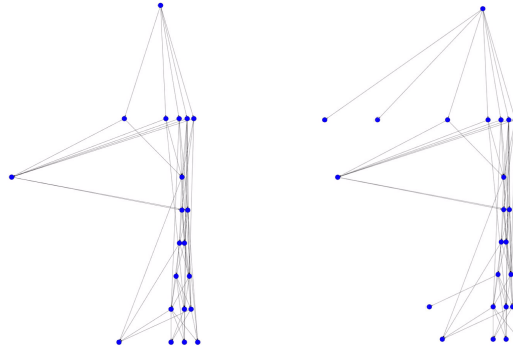


Example 1 – Add 3 Node

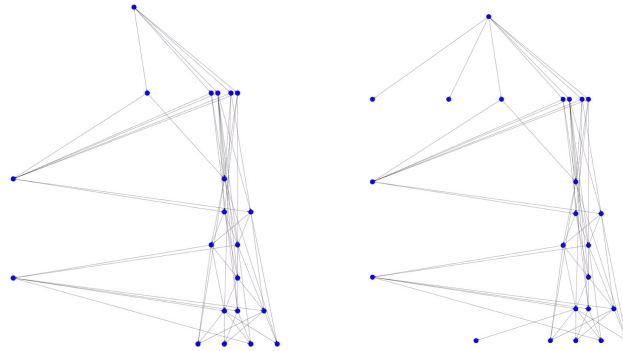


WS3
Base
Graph
1

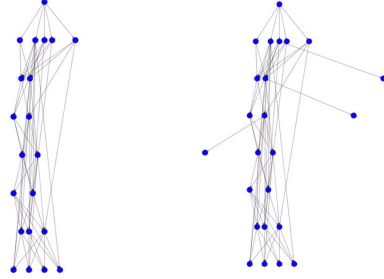
Example 2 – Add 3 Node



Example 3 – Add 3 Node

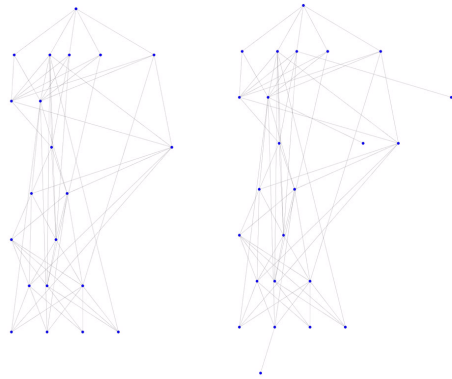


Example 1 – Add 3 Node

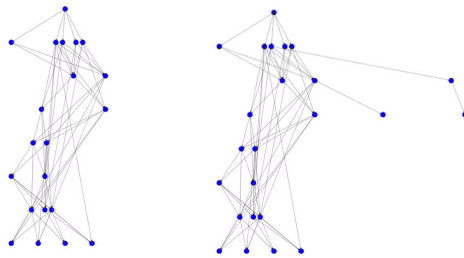


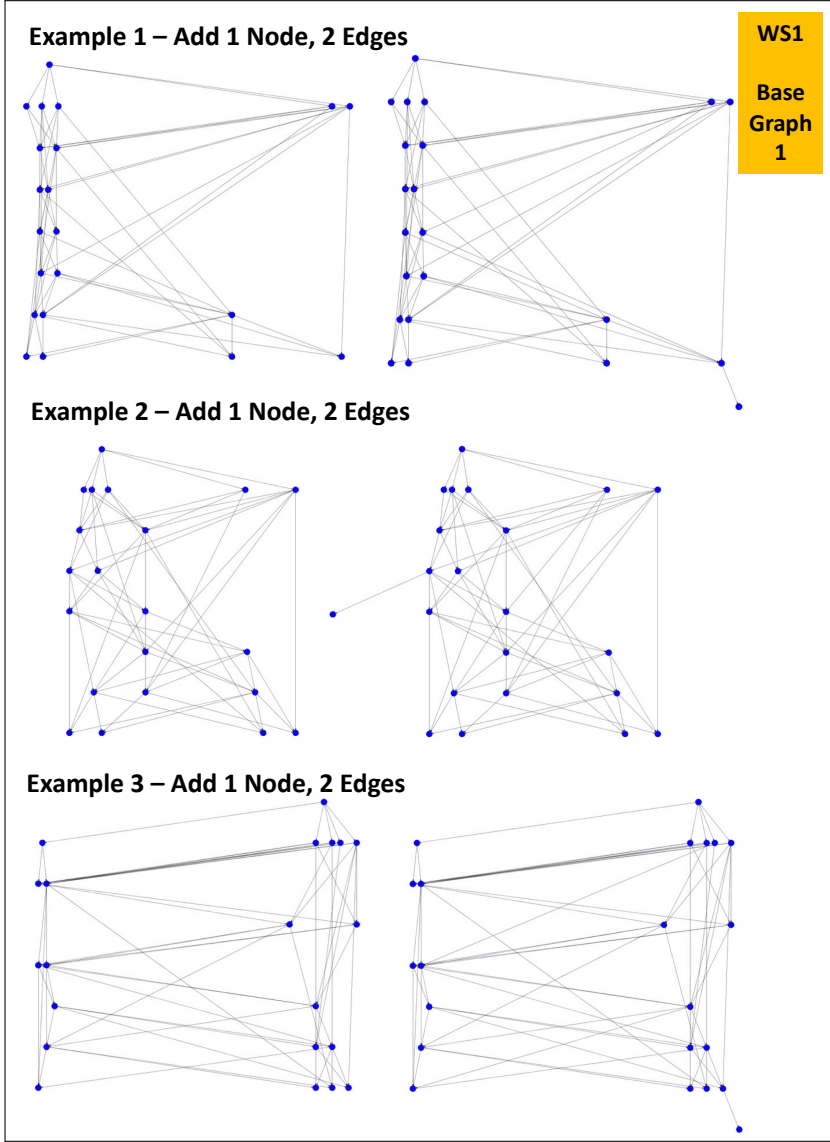
WS4
Base
Graph
1

Example 2 – Add 3 Node

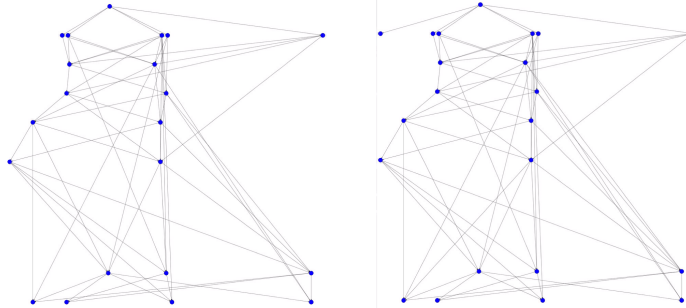


Example 3 – Add 3 Node



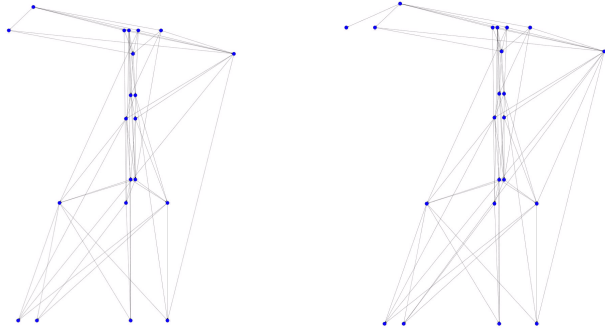


Example 1 – Add 1 Node, 2 Edges

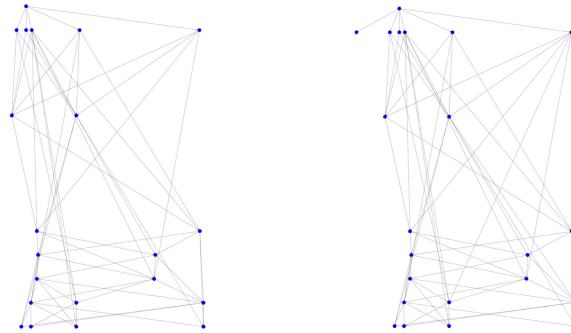


WS3
Base
Graph
1

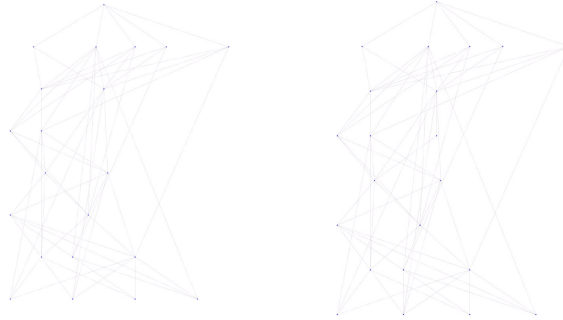
Example 2 – Add 1 Node, 2 Edges



Example 3 – Add 1 Node, 2 Edges

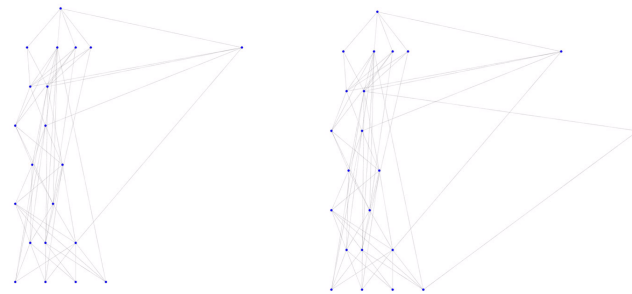


Example 1 – Add 1 Node, 2 Edges

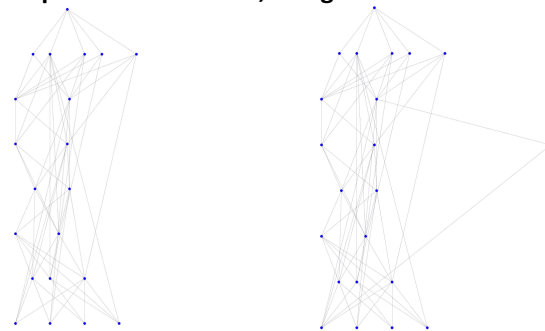


WS4
Base
Graph
1

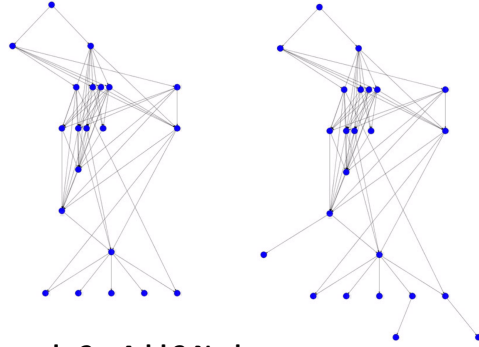
Example 2 – Add 1 Node, 2 Edges



Example 3 – Add 1 Node, 2 Edges

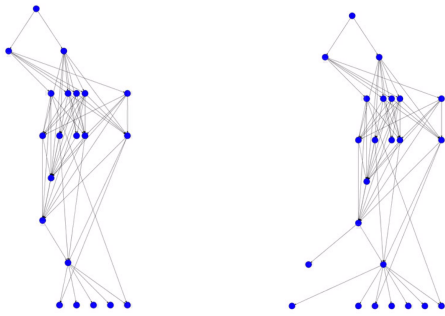


Example 1 – Add 3 Node

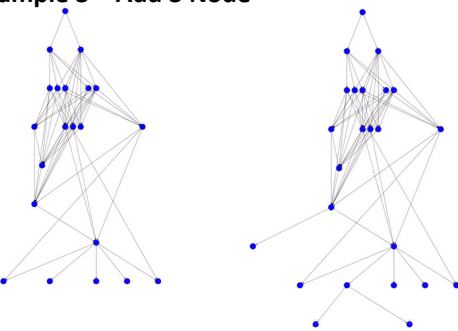


WS1
Base
Graph
2

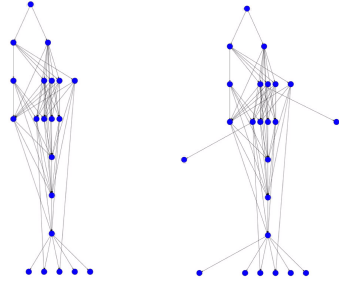
Example 2 – Add 3 Node



Example 3 – Add 3 Node

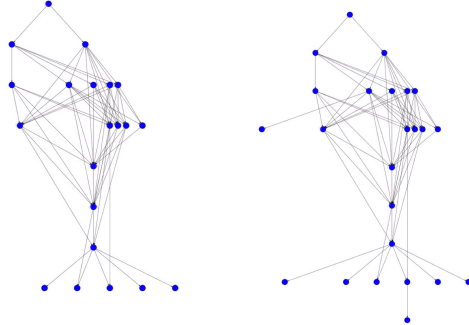


Example 1 – Add 3 Node

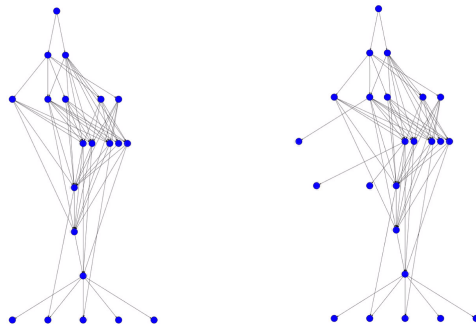


WS3
Base
Graph
2

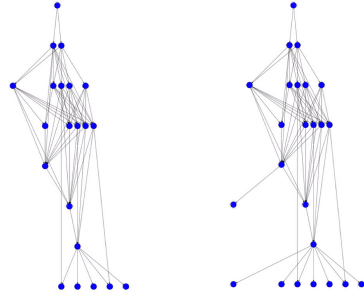
Example 2 – Add 3 Node



Example 3 – Add 3 Node

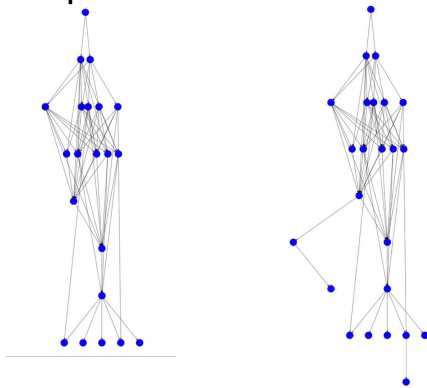


Example 1 – Add 3 Node

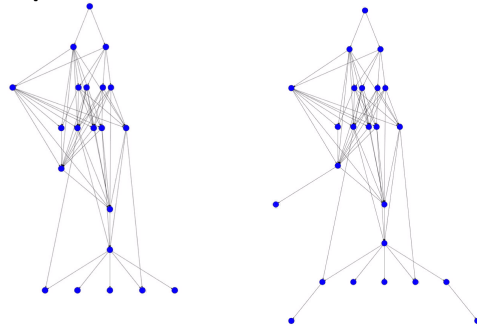


WS4
Base
Graph
2

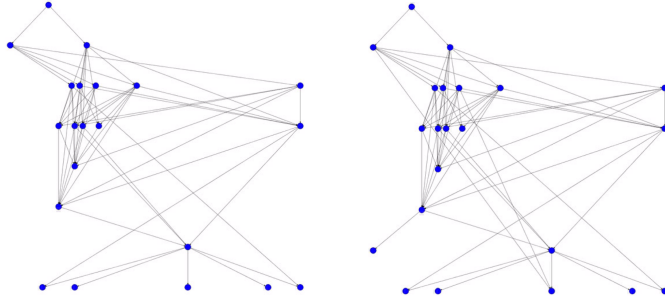
Example 2 – Add 3 Node



Example 3 – Add 3 Node

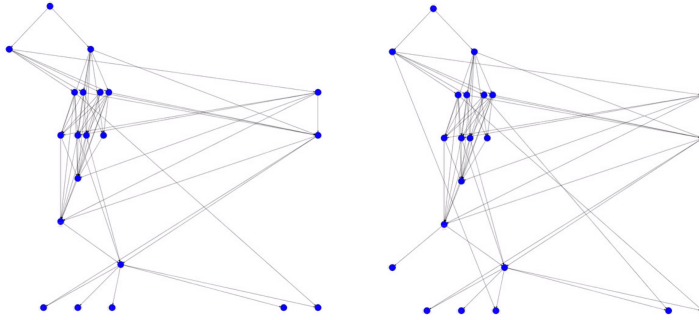


Example 1 – Add 1 Node, 2 Edges

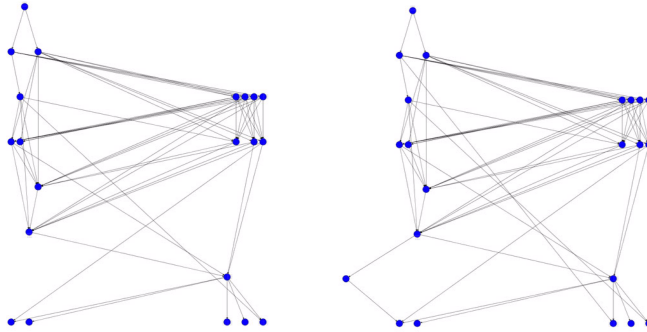


WS1
Base
Graph
2

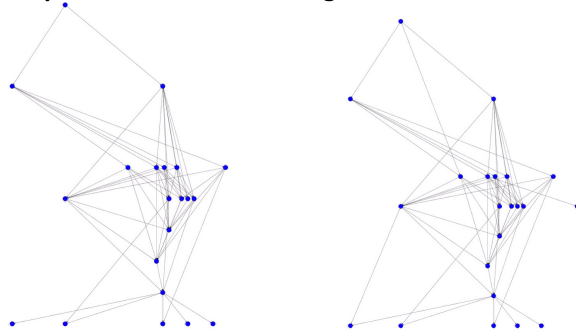
Example 2 – Add 1 Node, 2 Edges



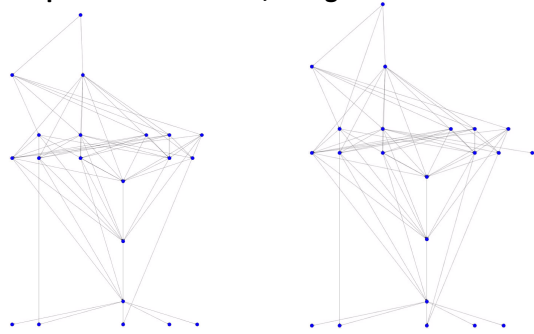
Example 3 – Add 1 Node, 2 Edges



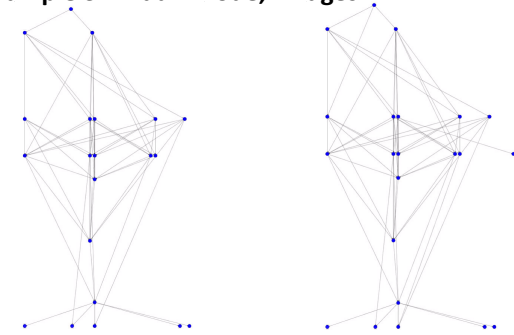
Example 1 – Add 1 Node, 2 Edges



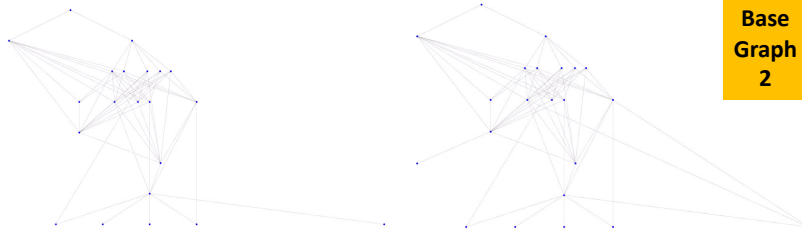
Example 2 – Add 1 Node, 2 Edges



Example 3 – Add 1 Node, 2 Edges



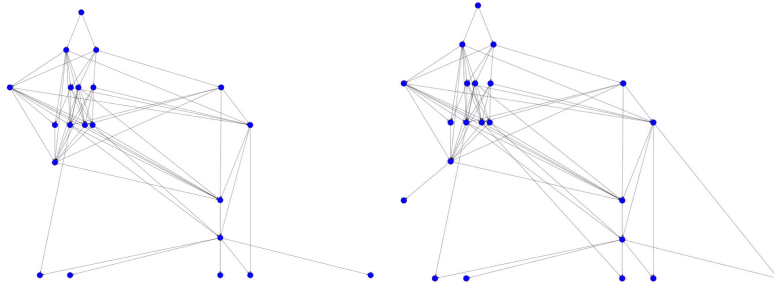
Example 1 – Add 1 Node, 2 Edges



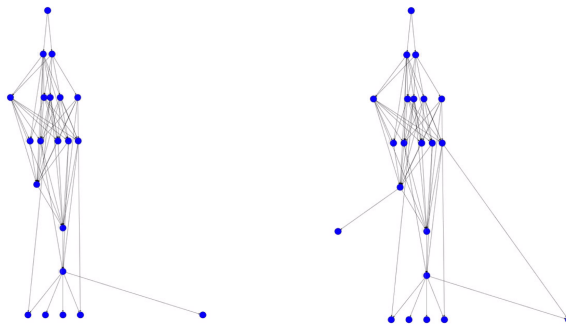
WS4

Base
Graph
2

Example 2 – Add 1 Node, 2 Edges



Example 3 – Add 1 Node, 2 Edges



1.5 Conclusion, and Future Work

Given the results, we can draw the final conclusion that our newly introduced drawing criteria for

- outwardly swapping as many graph changes as possible
- changing the outer hull by repositioning the outwardly swapped DAG changes
- dealing with DAG changes which are not possible to outwardly swap – nevertheless we also need a change of the DAG’s shape for those as well

are successful (keyword: percentage of outperforming the base implementation) and in spite of their intensive interventions in the drawing of the DAGs the resulting drawn DAGs still achieve more than 90% of the aesthetic criteria average compared to the base implementation. This means that our new criteria are intensive interventions and they break with the drawing conventions to some extent but they are still within the conventions which determine whether a human would like a visualization and find it aesthetically pleasing – otherwise the aesthetic criteria average would not be that good. Because of that and due to the feedback of our participants we can deduce that humans can work with our visualized DAGs and profit from the easier detectability of DAG changes.

In the future it would be interesting to further fine tune our layout’s parameters with respect to human perception. This would enable humans to spot differences in pairwise comparisons even better. This requires multiple user studies with an extensive number of participants making it a separate future work topic.

Also the positioning of the change within the enhanced white space is an improvement point in the future. If we were able to steer the position of the inner graph change into the center of the white space the chances of the graph change being spotted by a human would increase (our hypothesis). To achieve this an approach for balancing the size of the minimum (`CircleMin`) and the maximum (`CircleMax`) circle adjacent to the graph change is necessary (cf. Figure 16). This encompasses the development of a new algorithm and parameter tuning which makes it subject to future work.

Further, an analysis on specific graph properties and our shape change enhancements is for sure valuable in the future. This would provide in in-depth characterization for which DAGs our layout is particularly suitable, where performance drops need to be expected, and even if it would be advisable to invent further criteria for specific cases. This would be a suitable guidance for a future user of our layout. He would be spared of time-consuming try an error attempts. As it is the case for every layout - no layout is equally suitable for all graph types and properties.

Acknowledgements

We greatly benefited from the feedback of Prof. Günther Wallner. We would like to thank you very much for this.

References

- [1] S. E. Abdelhamid, C. J. Kuhlman, M. V. Marathe, and S. S. Ravi. Interactive exploration and understanding of contagion dynamics in networked populations. In *2016 International Conference on Behavioral, Economic and Socio-cultural Computing (BESC)*, pages 1–6. IEEE, 2016. doi:10.1109/BESC.2016.7804480.
- [2] V. Agafonkin, D. Carriere, M. Hataák, J. Kvam, J. Firebaugh, E. Locke, A. Harvey, J. Larsson, et al. polylabel – an iterative grid algorithm for approximating the centroid of an arbitrary polygon. GitHub.
- [3] D. Albers, M. Correll, and M. Gleicher. Task-driven evaluation of aggregation in time series visualization. In *Proceedings of the SIGCHI Conference on Human Factors in Computing Systems*, pages 551–560. Association for Computing Machinery, 2014. doi:10.1145/2556288.2557200.
- [4] D. Archambault and H. C. Purchase. The mental map and memorability in dynamic graphs. In *2012 IEEE Pacific Visualization Symposium*, pages 89–96. IEEE, 2012.
- [5] D. Archambault and H. C. Purchase. The “map” in the mental map: Experimental results in dynamic graph drawing. *International Journal of Human-Computer Studies*, 71(11):1044–1055, 2013. doi:10.1016/j.ijhcs.2013.08.004.
- [6] D. Archambault and H. C. Purchase. Mental map preservation helps user orientation in dynamic graphs. In W. Didimo and M. Patrignani, editors, *Graph Drawing*, pages 475–486. Springer Berlin Heidelberg, 2013.
- [7] D. Archambault and H. C. Purchase. Can animation support the visualisation of dynamic graphs? *Information Sciences*, 330:495–509, 2016.
- [8] D. Archambault and H. C. Purchase. On the effective visualisation of dynamic attribute cascades. *Information Visualization*, 15(1):51–63, 2016.
- [9] D. Archambault, H. C. Purchase, and B. Pinaud. Animation, small multiples, and the effect of mental map preservation in dynamic graphs. *IEEE Transactions on Visualization and Computer Graphics*, 17(4):539–552, 2011.
- [10] J. Avbelj, R. Müller, and R. Bamler. A metric for polygon comparison and building extraction evaluation. *IEEE Geoscience and Remote Sensing Letters*, 12(1):170–174, 2015.

- [11] K. Ballweg, M. Pohl, G. Wallner, and T. von Landesberger. Visual similarity perception of directed acyclic graphs: A study on influencing factors. In F. Frati and K.-L. Ma, editors, *Graph Drawing and Network Visualization*, pages 241–255. Springer International Publishing, 2018.
- [12] K. Ballweg, M. Pohl, G. Wallner, and T. von Landesberger. Visual similarity perception of directed acyclic graphs: A study on influencing factors and similarity judgment strategies. *Journal of Graph Algorithms and Applications*, 22(3):519–553, 2018. doi:10.7155/jgaa.00467.
- [13] F. Beck, M. Burch, S. Diehl, and D. Weiskopf. A taxonomy and survey of dynamic graph visualization. *Computer Graphics Forum*, 36(1):133–159, 2017. arXiv:<https://onlinelibrary.wiley.com/doi/pdf/10.1111/cgf.12791>, doi:10.1111/cgf.12791.
- [14] M. Behrisch, B. Bach, M. Hund, M. Delz, L. Von Rüden, J.-D. Fekete, and T. Schreck. Magnostics: Image-based search of interesting matrix views for guided network exploration. *IEEE Transactions on Visualization and Computer Graphics*, 23(1):31–40, 2017. doi:10.1109/TVCG.2016.2598467.
- [15] C. Bennett, J. Ryall, L. Spalteholz, and A. Gooch. The aesthetics of graph visualization. *Computational aesthetics*, 2007:57–64, 2007.
- [16] J. Bertin. *Semiology of Graphics*. University of Wisconsin Press, 1983.
- [17] J. Borge-Holthoefer, R. A. Baños, S. González-Bailón, and Y. Moreno. Cascading behaviour in complex socio-technical networks. *Journal of Complex Networks*, 1(1):3–24, 2013.
- [18] U. Brandes and M. Mader. A quantitative comparison of stress-minimization approaches for offline dynamic graph drawing. In M. van Kreveld and B. Speckmann, editors, *Graph Drawing*, pages 99–110, Berlin, Heidelberg, 2012. Springer Berlin Heidelberg.
- [19] M. Burch, G. Andrienko, N. Andrienko, M. Höferlin, M. Raschke, and D. Weiskopf. Visual task solution strategies in tree diagrams. In *2013 IEEE Pacific Visualization Symposium*, pages 169–176. IEEE, 2013.
- [20] M. Burch, N. Konevtsova, J. Heinrich, M. Hoferlin, and D. Weiskopf. Evaluation of traditional, orthogonal, and radial tree diagrams by an eye tracking study. *IEEE Transactions on Visualization and Computer Graphics*, 17(12):2440–2448, 2011. doi:10.1109/TVCG.2011.193.
- [21] M. Burch and D. Weiskopf. Visualizing dynamic quantitative data in hierarchies. In *Proceedings of International Conference on Information Visualization Theory and Applications*, pages 177–186. SCITEPRESS, 2011.
- [22] L. Chum-Cheng and Y. Hsu-Chun. On balloon drawings of rooted trees. *Journal of Graph Algorithms and Applications*, 11(2):431–452, 2007. doi:10.7155/jgaa.00153.

- [23] M. K. Coleman and D. S. Parker. Aesthetics-based graph layout for human consumption. *Software: Practice and Experience*, 26(12):1415–1438, 1996.
- [24] G. Di Battista, P. Eades, R. Tamassia, and I. G. Tollis. *Graph drawing: algorithms for the visualization of graphs*. Prentice Hall PTR, 1998.
- [25] S. Diehl and C. Görg. Graphs, They Are Changing. In *International Symposium on Graph Drawing*, pages 23–31. Springer, 2002. doi:10.1007/3-540-36151-0{_}3.
- [26] S. Diehl, C. Görg, and A. Kerren. Preserving the mental map using foresighted layout. In D. S. Ebert, J. M. Favre, and R. Peikert, editors, *Data Visualization 2001*, pages 175–184. Springer Vienna, 2001.
- [27] C. Dunne, S. I. Ross, B. Shneiderman, and M. Martino. Readability metric feedback for aiding node-link visualization designers. *IBM Journal of Research and Development*, 59(2-3):1–16, 2015. doi:10.1147/JRD.2015.2411412.
- [28] T. Dwyer, B. Lee, D. Fisher, K. I. Quinn, P. Isenberg, G. Robertson, and C. North. A comparison of user-generated and automatic graph layouts. *IEEE Transactions on Visualization and Computer Graphics*, 15(6):961–968, 2009. doi:10.1109/TVCG.2009.109.
- [29] P. Eades. Drawing free trees. *Bulletin of the Institute for Combinatorics and its Applications*, 5:10–36, 1992.
- [30] P. Eades, S.-H. Hong, K. Klein, and A. Nguyen. Shape-based quality metrics for large graph visualization. In E. Di Giacomo and A. Lubiw, editors, *Graph Drawing and Network Visualization*, pages 502–514. Springer International Publishing, 2015.
- [31] P. Eades, W. Lai, K. Misue, and K. Sugiyama. Preserving the mental map of a diagram. In *Proceedings of Compugraphics '91*, pages 24–33, 1991.
- [32] H. Edelsbrunner. Alpha shapes – a survey. *Tessellations in the Sciences*, 27:1–25, 2010.
- [33] H. Edelsbrunner, D. G. Kirkpatrick, and R. G. Seidel. On the shape of a set of points in the plane. *IEEE Transactions on Information Theory*, 29(4):551–559, 1983. doi:10.1109/TIT.1983.1056714.
- [34] K. Egberg Thyme, B. Wiberg, B. Lundman, and U. H. Graneheim. Qualitative content analysis in art psychotherapy research: Concepts, procedures, and measures to reveal the latent meaning in pictures and the words attached to the pictures. *The Arts in Psychotherapy*, 40(1):101–107, 2013.
- [35] S. I. Fabrikant and D. R. Montello. The effect of instructions on distance and similarity judgements in information spatializations. *International Journal of Geographical Information Science*, 22(4):463–478, 2008. arXiv:<https://doi.org/10.1080/13658810701517096>, doi:10.1080/13658810701517096.

- [36] S. L. Franconeri. The nature and status of visual resources. *The Oxford Handbook of Cognitive Psychology*, pages 1–19, 2014. doi:10.1093/oxford/hb/9780195376746.013.0010.
- [37] J. Fuchs, P. Isenberg, A. Bezerianos, F. Fischer, and E. Bertini. The influence of contour on similarity perception of star glyphs. *IEEE Computer Graphics and Applications*, 20(12):2251–2260, 2014. doi:10.1109/TVCG.2014.2346426.
- [38] D. Garcia-Castellanos and U. Lombardo. Poles of inaccessibility: A calculation algorithm for the remotest places on earth. *Scottish Geographical Journal*, 123(3):227–233, 2007. doi:10.1080/14702540801897809.
- [39] C. Geffers and P. Gastmeier. Nosocomial Infections and Multidrug-resistant Organisms in Germany. *Deutsches Ärzteblatt International*, 108(6):87–93, 2011.
- [40] S. Ghani, N. Elmqvist, and J. S. Yi. Perception of animated node-link diagrams for dynamic graphs. *Computer Graphics Forum*, 31(3pt3):1205–1214, 2012. doi:10.1111/j.1467-8659.2012.03113.x.
- [41] R. L. Graham. An efficient algorithm for determining the convex hull of a finite planar set. *Information Processing Letters*, 1(4):132–133, 1972.
- [42] S. Grivet, D. Auber, J.-P. Domenger, and G. Melançon. *Bubble tree drawing algorithm*, pages 633–641. Springer Netherlands, 2006. doi:10.1007/1-4020-4179-9_91.
- [43] B. Haarbrandt, B. Schreiweis, S. Rey, U. Sax, S. Scheithauer, O. Rienhoff, P. Knaup-Gregori, U. Bavendiek, C. Dieterich, B. Brors, et al. Highmed—an open platform approach to enhance care and research across institutional boundaries. *Methods of information in medicine*, 57(S 01):66–81, 2018.
- [44] W. Huang, J. Luo, T. Bednarz, and H. Duh. Making graph visualization a user-centered process. *Journal of Visual Languages & Computing*, 48:1–8, 2018.
- [45] D. P. Huttenlocher, G. A. Klanderma, and W. J. Rucklidge. Comparing images using the hausdorff distance. *IEEE Transactions on Pattern Analysis and Machine Intelligence*, 15(9):850–863, 1993. doi:10.1109/34.232073.
- [46] T. Kalbe, T. Tekušová, T. Schreck, and F. Zeilfelder. Gpu-accelerated 2d point cloud visualization using smooth splines for visual analytics applications. In *Proceedings of the 24th Spring Conference on Computer Graphics*, pages 97–104. Association for Computing Machinery, 2008. doi:10.1145/1921264.1921286.
- [47] M. Kaufmann and D. Wagner. *Drawing graphs: methods and models*, volume 2025. Springer, 2003.

- [48] N. Kerracher, J. B. Kennedy, and K. Chalmers. Using a Task Classification in the Visualisation Design Process for Task Understanding and Abstraction: an Empirical Study. In J. Johansson, F. Sadlo, and T. Schreck, editors, *EuroVis 2018 - Short Papers*. The Eurographics Association, 2018. doi:10.2312/eurovisshort.20181082.
- [49] A. Kerren and F. Schreiber. Network visualization for integrative bioinformatics. In *Approaches in Integrative Bioinformatics*, pages 173–202. Springer, 2014.
- [50] S. Kieffer, T. Dwyer, K. Marriott, and M. Wybrow. HOLA: Human-like orthogonal network layout. *IEEE Transactions on Visualization and Computer Graphics*, 22(1):349–358, 2016. doi:10.1109/TVCG.2015.2467451.
- [51] Y. Kim and J. Heer. Assessing effects of task and data distribution on the effectiveness of visual encodings. *Computer Graphics Forum*, 37(3):157–167, 2018. doi:10.1111/cgf.13409.
- [52] S. Klettner. Why shape matters – on the inherent qualities of geometric shapes for cartographic representations. *ISPRS International Journal of Geo-Information*, 8(5), 2019. doi:10.3390/ijgi8050217.
- [53] A. Klippel, F. Hardisty, R. Li, and C. Weaver. Colour-enhanced star plot glyphs: Can salient shape characteristics be overcome? *Cartographica: The International Journal for Geographic Information and Geovisualization*, 44(3):217–231, 2009. arXiv:<https://doi.org/10.3138/carto.44.3.217>, doi:10.3138/carto.44.3.217.
- [54] A. Klippel, F. Hardisty, and C. Weaver. Star plots: How shape characteristics influence classification tasks. *Cartogr. Geogr. Inf. Sci.*, 36(2):149–163, 2009. doi:10.1559/152304009788188808.
- [55] S. G. Kobourov, T. Mchedlidze, and L. Vonessen. Gestalt principles in graph drawing. In E. Di Giacomo and A. Lubiw, editors, *Graph Drawing and Network Visualization*, pages 558–560. Springer International Publishing, 2015.
- [56] S. G. Kobourov, S. Pupyrev, and B. Saket. Are crossings important for drawing large graphs? In C. Duncan and A. Symvonis, editors, *Graph Drawing: 22nd International Symposium, GD 2014*, pages 234–245. Springer, 2014. doi:10.1007/978-3-662-45803-7_20.
- [57] E. Kypridemou, M. Zito, and M. Bertamini. The Effect of Graph Layout on the Perception of Graph Properties. In A. Kerren, C. Garth, and G. E. Marai, editors, *EuroVis 2020 - Short Papers*. The Eurographics Association, 2020. doi:10.2312/evs.20201039.
- [58] O. Lenz, F. Keul, S. Bremm, K. Hamacher, and T. von Landesberger. Visual analysis of patterns in multiple amino acid mutation graphs. In

- IEEE Conference on Visual Analytics Science and Technology, 2014. VAST 2014*, pages 93–102. IEEE, 2014. doi:10.1109/VAST.2014.7042485.
- [59] C.-C. Lin, W. Huang, W.-Y. Liu, and C.-Y. Chen. On aesthetics for user-sketched layouts of vertex-weighted graphs. *Journal of Visualization*, 24(1):157–171, 2021. doi:10.1007/s12650-020-00695-2.
- [60] C.-C. Lin, W. Huang, W.-Y. Liu, and W.-L. Chen. Evaluating aesthetics for user-sketched layouts of symmetric graphs. *Journal of Visual Languages & Computing*, 48:123–133, 2018. URL: <https://www.sciencedirect.com/science/article/pii/S1045926X18301204>, doi:<https://doi.org/10.1016/j.jvlc.2018.08.004>.
- [61] W. Liu and S. Zhong. A novel dynamic model for web malware spreading over scale-free networks. *Physica A: Statistical Mechanics and its Applications*, 505:848–863, 2018.
- [62] E. Mäkinen and H. Siirtola. The barycenter heuristic and the reorderable matrix. *Informatika (Slovenia)*, 29(3):357–364, 2005.
- [63] K. Misue, P. Eades, W. Lai, and K. Sugiyama. Layout adjustment and the mental map. *Journal of Visual Languages & Computing*, 6(2):183–210, 1995.
- [64] J. R. Munkres. *Elements of algebraic topology*. CRC Press, 2019.
- [65] A. V. Pandey, J. Krause, C. Felix, J. Boy, and E. Bertini. Towards understanding human similarity perception in the analysis of large sets of scatter plots. In *Proceedings of the 2016 CHI Conference on Human Factors in Computing Systems*, pages 3659–3669. Association for Computing Machinery, 2016. doi:10.1145/2858036.2858155.
- [66] F. N. Paulisch and W. F. Tichy. EDGE: An extendible graph editor. *Software: Practice and Experience*, 20(S1):63–88, 1990. doi:10.1002/spe.4380201307.
- [67] H. C. Purchase. Which aesthetic has the greatest effect on human understanding? In G. DiBattista, editor, *Graph Drawing: 5th International Symposium, GD 1997*, pages 248–261. Springer, 1997. doi:10.1007/3-540-63938-1_67.
- [68] H. C. Purchase. Metrics for graph drawing aesthetics. *Journal of Visual Languages & Computing*, 13(5):501–516, 2002. doi:10.1006/S1045-926x(02)00016-2.
- [69] H. C. Purchase, R. F. Cohen, and M. James. Validating graph drawing aesthetics. In F. J. Brandenburg, editor, *Graph Drawing*, pages 435–446. Springer Berlin Heidelberg, 1996.

- [70] H. C. Purchase, C. Pilcher, and B. Plimmer. Graph drawing aesthetics – created by users, not algorithms. *IEEE Transactions on Visualization and Computer Graphics*, 18(1):81–92, 2012. doi:10.1109/TVCG.2010.269.
- [71] H. C. Purchase and A. Samra. Extremes are better: Investigating mental map preservation in dynamic graphs. In *International Conference on Theory and Application of Diagrams*, pages 60–73. Springer Berlin Heidelberg, 2008.
- [72] R. Reber. Reasons for preference for symmetry. *Behavioral and Brain Sciences*, 25(3):415, 2002.
- [73] F. D. Sahneh, A. Vajdi, H. Shakeri, F. Fan, and C. Scoglio. GEMFsim: a stochastic simulator for the generalized epidemic modeling framework. *Journal of Computational Science*, 22:36–44, 2017.
- [74] J. Saldaña. *The Coding Manual for Qualitative Researchers*. SAGE Publications, 2 edition, 2012.
- [75] P. Sarlin. Macroprudential oversight, risk communication and visualization. *Journal of Financial Stability*, 27:160–179, 2016.
- [76] M. Schäpers. *An improved directed acyclic graph layout algorithm for visual comparison considering the directed acyclic graph’s shape*. Master’s thesis, Technical University Darmstadt, 2019.
- [77] T. Schreck and C. Panse. A new metaphor for projection-based visual analysis and data exploration. In R. F. Erbacher, J. C. Roberts, M. T. Gröhn, and K. Börner, editors, *Visualization and Data Analysis 2007*, pages 200 – 211. SPIE, 2007.
- [78] T. Schreck, M. Schüßler, F. Zeilfelder, and K. Worm. Butterfly plots for visual analysis of large point cloud data. In *WSCG 2008: Full Papers: The 16-th International Conference in Central Europe on Computer Graphics, Visualization and Computer Vision in Co-Operation with EUROGRAPH-ICS*, pages 30–40. Václav Skala - UNION Agency, 2008.
- [79] M. Schreier. *Qualitative Content Analysis in Practice*. SAGE Publications, 2012.
- [80] M. Siebenhaller, S. S. Nielsen, F. McGee, I. Balaur, C. Auffray, and A. Mazein. Human-like layout algorithms for signalling hypergraphs: outlining requirements. *Briefings in Bioinformatics*, 21(1):62–72, 2018. doi:10.1093/bib/bby099.
- [81] P. Simonetto, D. Archambault, and S. Kobourov. Event-based dynamic graph visualisation. *IEEE Transactions on Visualization and Computer Graphics*, 26(7):2373–2386, 2020. doi:10.1109/TVCG.2018.2886901.

- [82] K. Sugiyama, S. Tagawa, and M. Toda. Methods for visual understanding of hierarchical system structures. *IEEE Transactions on Systems, Man, and Cybernetics*, 11(2):109–125, 1981.
- [83] R. Tamassia. *Handbook of graph drawing and visualization*. CRC press, 2013.
- [84] The JUNG Framework Development Team. Jung – java universal network/graph framework [online]. URL: <http://jung.sourceforge.net> [cited 2021/10/10].
- [85] F. van Ham and B. Rogowitz. Perceptual organization in user-generated graph layouts. *IEEE Transactions on Visualization and Computer Graphics*, 14(6):1333–1339, 2008.
- [86] F. Viégas, M. Wattenberg, J. Hebert, G. Borggaard, A. Cichowlas, J. Feinberg, J. Orwant, and C. Wren. Google+ ripples: A native visualization of information flow. In *International Conference on World Wide Web*, pages 1389–1398. Association for Computing Machinery, 2013.
- [87] T. von Landesberger, S. Diel, S. Bremm, and D. W. Fellner. Visual analysis of contagion in networks. *Information Visualization*, 14(2):93–110, 2015. doi:10.1177/1473871613487087.
- [88] L. Wilkinson, A. Anand, and r. Grossman. Graph-theoretic scagnostics. In *IEEE Symposium on Information Visualization, 2005. INFOVIS 2005.*, pages 157–164. IEEE, 2005. doi:10.1109/INFVIS.2005.1532142.
- [89] M. Wunderlich, I. Block, T. von Landesberger, M. Petzold, M. Marschollek, and S. Scheithauer. Visual Analysis of Probabilistic Infection Contagion in Hospitals. In H.-J. Schulz, M. Teschner, and M. Wimmer, editors, *Vision, Modeling and Visualization*. The Eurographics Association, 2019. doi:10.2312/vmv.20191328.
- [90] J. Zhao, N. Cao, Z. Wen, Y. Song, Y.-R. Lin, and C. Collins. # fluxflow: Visual analysis of anomalous information spreading on social media. *IEEE Transactions on Visualization and Computer Graphics*, 20(12):1773–1782, 2014.